

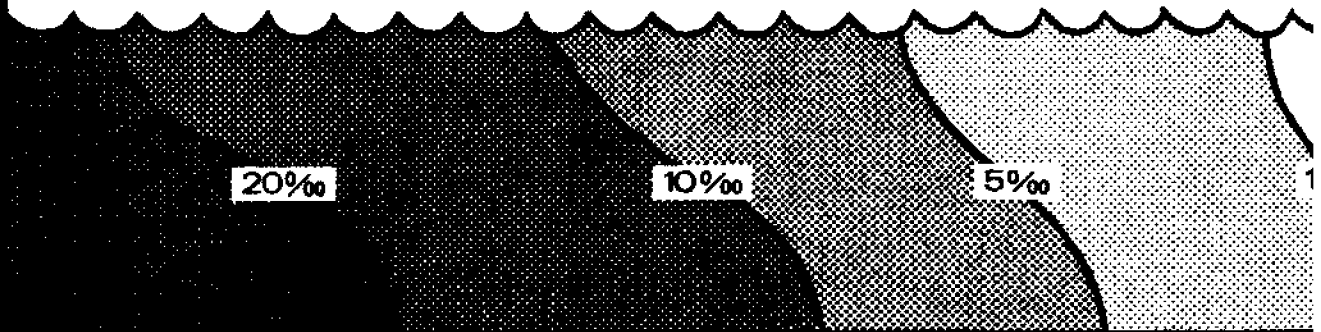
CIRCULATING COPY
Sea Grant Depository

A Model of Salt Intrusion in a Partially Mixed Estuary

by

James E. Overland

LOAN COPY ONLY



NEW YORK INSTITUTE OF OCEAN RESOURCES

New York Institute of Ocean Resources
39 East Tenth Street
New York, New York 10003

CIRCULATING COPY
Sea Grant Depository

A MODEL OF SALT INTRUSION IN A
PARTIALLY MIXED ESTUARY

by

James E. Overland

Research supported by the ARCA Foundation and by the
Office of Sea Grant, National Oceanic and Atmospheric
Administration, United States Department of Commerce

Technical Report 73-1

September 1973

TABLE OF CONTENTS

| | Page |
|---|------|
| SUMMARY | i |
| LIST OF FIGURES | iv |
| ACKNOWLEDGMENTS | vi |
| I. INTRODUCTION | 1 |
| A. Dispersion versus diffusion | 4 |
| B. The basis of the proposed model and review of previous work | 6 |
| II. MATHEMATICAL FORMULATION | 8 |
| A. Governing equations | 18 |
| B. Simplification of the general equations | 13 |
| C. Final formulation | 15 |
| D. Boundary conditions | 16 |
| E. Turbulent processes | 18 |
| III. METHOD OF SOLUTION | 26 |
| IV. RESULTS | 32 |
| V. EXAMPLES OF POLLUTANT LOADING | 58 |
| VI. CONCLUSION | 68 |
| REFERENCES | 71 |

SUMMARY

A model is developed for salt intrusion in partially mixed estuaries that specifies the vertical and horizontal distribution of salinity and volume transport in response to run-off and mixing assumptions. An estimate is made of the dispersion of a pollutant by the calculated velocity distribution in the intrusion region. The model is accessible to further refinement for use in specific estuaries.

The salt flux through any cross section is shown to be composed of a freshwater component, a dispersive mode resulting from density-induced flow, a dispersive mode of tidal mixing, and a diffusive mode resulting from turbulent mixing. The diffusive mode arises from the correlation of random turbulent fluctuations, while the dispersive modes arise from cross sectional averaging of deterministic variables.

The coupled salt and momentum equations in a vorticity-stream function formulation are solved on a numerical grid that resolves one meter in the vertical and six kilometers in the horizontal. The major dynamic simplification is specification of the channel as narrow. For the cases studied, it was assumed further that the density-induced flow predominated over tidal mixing as an intrusion mechanism. The major intent is to calculate directly the differential advection of salt from the vertical profiles of the horizontal currents, avoiding the necessity of parameterizing the advective circulation with a horizontal dispersion coefficient. The time step restriction of the small vertical grid interval was removed by treating all points in a vertical column implicitly. The system was solved by a Gaussian elimination technique.

Thirteen examples were run to assess the effects of river discharge, wind, and various assumptions of vertical turbulent mixing. The characteristic estuary dimensions and parameters are from the Hudson River. A constant depth of 14 meters and a constant width of 1040 meters were used throughout, although the formulation can accommodate horizontal variations in these dimensions. Four cases were run with constant values of the vertical eddy viscosity, A , and diffusivity, K_z , assuming a run-off of $212.4 \text{ m}^3/\text{sec}$. With $A = K_z = 4 \text{ cm}^2/\text{sec}$, the 0.1‰ isohaline was located 138 kilometers from the seaward boundary where fixed values of salinity were maintained. The distance for $10 \text{ cm}^2/\text{sec}$ values was 72 km and the distance for $25 \text{ cm}^2/\text{sec}$ was 60 km. The vertical variation of the salt profiles decreased with increasing eddy diffusivity. When $K_z = 4 \text{ cm}^2/\text{sec}$ and $A = 8 \text{ cm}^2/\text{sec}$, the intrusion length was 96 km, indicating that the dynamic balance is important in determining intrusion length.

Variable coefficients were also investigated. The coefficients consisted of an adiabatic mixing coefficient with a maximum, KM , that decreased toward the bottom and surface, modified by a separate Richardson number dependence for the eddy viscosity and the eddy diffusivity. It was assumed that the generation of turbulence is not related to the tidal mean flow so that the Richardson number is a function of stability only. In an example in which the depth but not the stability dependence was used, velocity magnitudes within the intrusion region were considerably different from those of the constant coefficient cases, indicating that replacing depth variable coefficients by virtual constant coefficients will not produce similar results.

The use of stability dependence makes a qualitative improvement over

constant coefficient cases by tending to form a stronger halocline near mid-depth. Results for different values of KM , considered proportional to the intensity of tidally generated turbulence, suggest that for large adiabatic values, $KM = 20 \text{ cm}^2/\text{sec}$, the eddy diffusivities remain large, while for lower values, $KM = 10 \text{ cm}^2/\text{sec}$, the stability factors reduce the in situ value of the eddy coefficients to the values of 2 to $5 \text{ cm}^2/\text{sec}$ which are observed in partially mixed estuaries with less intense tidal mixing. With $KM = 10 \text{ cm}^2/\text{sec}$, a change in run-off from $99 \text{ m}^3/\text{sec}$ to $424 \text{ m}^3/\text{sec}$ produced a displacement in the limit of salt intrusion of 25 km. The results of the model suggest that the horizontal distribution of salinity in the Hudson River, under summer run-off conditions, is associated with high values of KM in agreement with the strong tidal currents of the Hudson.

The dispersion of a slug load and continuously released pollutant was calculated using the velocities and eddy diffusivities derived by the intrusion model for summer conditions. The circulation spreads the pollutant initially, then the pollutants recirculate seaward in the surface layer and return landward in the bottom layer. The apparent one dimensional horizontal dispersion coefficient estimated from the pollutant distribution in the model after seven days was $36 \times 10^5 \text{ cm}^2/\text{sec}$. This corresponds to a value estimated from a dye release in the Hudson River under similar conditions of 7 to $22 \times 10^5 \text{ cm}^2/\text{sec}$.

LIST OF FIGURES

- Figure 1. Specification of coordinate system.
- Figure 2. Solutions for constant eddy coefficient cases. (After Hansen and Rattray, 1965)
- Figure 3. Dependence of the ratio of eddy diffusivity to eddy viscosity upon Richardson number as hypothesized by Munk and Anderson (1948) and verified for the Mersey Estuary by Bowden and Gilligan (1971).
- Figure 4. Assumed vertical variation of eddy coefficients for neutral conditions.
- Figure 5. Specification of numerical grid.
- Figure 6. Case I. Constant coefficients, $K_z = A = 4 \text{ cm}^2/\text{sec}$; Run-off $212.4 \text{ m}^3/\text{sec}$.
- Figure 7. Case II. Constant coefficients, $K_z = 4 \text{ cm}^2/\text{sec}$; $A = 8 \text{ cm}^2/\text{sec}$; Run-off $212.4 \text{ m}^3/\text{sec}$.
- Figure 8. Case III. Constant coefficients, $K_z = A = 10 \text{ cm}^2/\text{sec}$; Run-off $212.4 \text{ m}^3/\text{sec}$.
- Figure 9. Case IV. Constant coefficients, $K_z = A = 25 \text{ cm}^2/\text{sec}$; Run-off $212.4 \text{ m}^3/\text{sec}$.
- Figure 10. Case V. Variable coefficients without stability dependence; $K_M = 10 \text{ cm}^2/\text{sec}$; Run-off $212.4 \text{ m}^3/\text{sec}$.
- Figure 11. Plot of salinity versus distance into the estuary for Cases I-V. Cases I-IV use increasing values of constant eddy coefficients. Case V includes depth dependence for coefficients, but is without stability effects.
- Figure 12. Case VI. Full model, $K_M = 10 \text{ cm}^2/\text{sec}$; Run-off $212.4 \text{ m}^3/\text{sec}$.
- Figure 13. Case VII. Full model $K_M = 15 \text{ cm}^2/\text{sec}$; Run-off $212.4 \text{ m}^3/\text{sec}$.
- Figure 14. Case VIII. Full model, $K_M = 20 \text{ cm}^2/\text{sec}$; Run-off $212.4 \text{ m}^3/\text{sec}$.
- Figure 15. Plot of salinity vs. distance into the estuary for Cases VI-VIII. These cases show the effect of varying the maximum eddy coefficient, K_M , on salt intrusion. Model run-off was 7500 cfs. Data is from Giese and Barr (1967).

- Figure 16. Case IX. Full model with low run-off. $KM = 10 \text{ cm}^2/\text{sec}$; Run-off $99.1 \text{ m}^3/\text{sec}$.
- Figure 17. Case X. Full model with high run-off. $KM = 10 \text{ cm}^2/\text{sec}$; Run-off $424.8 \text{ m}^3/\text{sec}$.
- Figure 18. Plot of salinity vs. distance into the estuary for Cases VI, IX, and X. $KM = 10 \text{ cm}^2/\text{sec}$. Run-off values of 99.1, 212.4, $424.8 \text{ m}^3/\text{sec}$.
- Figure 19. Case XI. Full model, $KM = 15 \text{ cm}^2/\text{sec}$; Run-off $141.6 \text{ m}^3/\text{sec}$.
- Figure 20. Case XII. Full model, $KM = 20 \text{ cm}^2/\text{sec}$; Run-off $141.6 \text{ m}^3/\text{sec}$.
- Figure 21. Plot of salinity vs. distance into the estuary for Cases XI and XII. Case XI assumed a value of $15 \text{ cm}^2/\text{sec}$ for KM and Case XII assumed $20 \text{ cm}^2/\text{sec}$. Run-off was 5000 cfs ($141.6 \text{ m}^3/\text{sec}$).
- Figure 22. Case XIII. Full model with application of a wind stress of 0.1 dyne/cm^2 in the upstream direction. $KM = 10 \text{ cm}^2/\text{sec}$; Run-off of $212.4 \text{ m}^3/\text{sec}$.
- Figure 23. Distribution of a conservative tracer for initial condition, one tidal cycle (12.42 hrs) after the initial condition and two cycles.
- Figure 24. Distribution of a conservative tracer for seven and fourteen tidal cycles and one month after the initial condition.
- Figure 25. Plot of dye mass per 6 kilometer segment for 1, 2, 7, 14, 28 tidal cycles after release.
- Figure 26. Amount of relative mass remaining in the system as a function of time.
- Figure 27. Results of continuous loading for 0.56, 3.3, and 9 days after initial insertion.

ACKNOWLEDGMENTS

The author is indebted to Dr. W. J. Pierson for his continuous encouragement and guidance throughout the course of this investigation. Dr. H. Friedrich contributed in many helpful discussions and the insight of Dr. G. Neumann and Dr. J. Spar was drawn upon throughout the investigation. I especially wish to express my thanks to Dr. H. R. Frey for his help in carrying out this project.

The author's interest and original background in estuary processes was obtained from Dr. M. Rattray, Jr. and Dr. G. Cannon as a student at the University of Washington.

I would also like to acknowledge the help of Mr. R. Stacy, Mr. D. Cavalieri, my wife, Doris, and my cat, Fritz, who aided in the preparation of the figures.

The major part of this research was performed at the Department of Meteorology and Oceanography, New York University; the project was transferred to the New York Institute of Ocean Resources during June 1973. The first 12 months of effort at N.Y.U. were supported by the ARCA Foundation. and the succeeding 9 months were supported by the Office of Sea Grant (Grant Number 04-3-158-32) with matching funds from the ARCA Foundation. The ARCA Foundation has supported the completion of the project at the New York Institute of Ocean Resources.

I. INTRODUCTION

"The estuary - septic tank of the megalopolis"

P. De Falco in Estuaries

Estuaries are zones of transition from an oceanic to a freshwater environment. In this region saline ocean water adjusts to fresh river water over oceanographically short horizontal distances on the scale of 200 kilometers or less. The mechanism of salt intrusion can be separated into a diffusion-like effect due to lateral and vertical shear of tidal currents, or more simply "tidal mixing", and a convective mode due to density effects.

In the lower reaches of most coastal plain estuaries of the East Coast of the United States, tidal mixing predominates because of the effects of wide shallow embayments and strong tidal currents. The large horizontal extent of these lower reaches allows lateral shear of the tidal current to develop, which, when averaged over a tidal cycle, may result in a net landward current in one region of the estuary which is balanced by a net seaward flow elsewhere. If the average salinity is higher in the landward flow, a net flux of salt into the estuary is produced.

Estuaries typically become narrow and deep farther upstream, reducing the cross-channel variation of the tidal currents. Tidal energy in this region may be insufficient to maintain vertical homogeneity and density effects may, accordingly, become more important. This transition represents the change from a well mixed estuary circulation to a partially mixed system. In the partially mixed region, seawater, being denser than the water of the river, flows into the estuary as a bottom layer, displacing the lighter less saline water. As the salt intrudes, it gradually mixes

upward, modifying the overlying seaward flowing surface layer. The convective circulation derived from this density flow is known as the gravitational circulation. Clearly, in some parts of an estuary, both salt intrusion mechanisms, tidal mixing and gravitational circulation, are acting simultaneously.

Freshwater outflow continually tends to flush salt out of the estuary to counteract the landward flux of salt from the diffusive and convective modes. An equilibrium distribution of salt is established when the net salt flux through all cross sections is zero. The limit of salt intrusion and the vertical variation of salt in the estuary are functions of the amount of fresh water influx, oceanic salinity, intensity of tidal action, wind stress, intensity of locally generated turbulence, and variations of width and bathymetry.

To provide a quantitative definition of these salt fluxes, the instantaneous horizontal velocity, u , is separated into a random turbulent component, u' , a tidal component, u_T , and a non-tidal mean velocity, u_M , such that

$$u \equiv u_M + u_T + u' \quad (1.1)$$

The concept of turbulent fluctuations implies that, for apparently similar external conditions, values for turbulent velocities u' are distributed according to a probability density function. It is thus necessary to define an averaging rule (E) such that when a velocity signal is averaged by this rule, the random fluctuations are filtered from the signal, leaving only the deterministic parts. Therefore, (E) should have the following property:

$$\langle u' \rangle_E = 0 \quad (1.2)$$

so that

$$\langle u \rangle_E = u_M + u_T \quad (1.3)$$

Equation (1.2) is satisfied exactly if (E) is taken as an average across an ensemble; that is, if one considered a large number of possible realizations of the flow field, u , the average value of all the realizations is the most probable value of u and is defined by (1.3). One could alternatively consider (E) to be a space or time average such that the averaging interval is large enough so that (1.2) is satisfied, but is much shorter than the length and time scales defined by the tidal period, T . The probability density function of u' may be considered to be a slowly varying function, however, so that an averaging interval t_0 , with $T \gg t_0$, can be found so that (1.2) is satisfied approximately for most naturally occurring conditions.

Decompose the salinity field, s , in a similar manner as the velocity field and define a cross-channel cross sectional average as $\langle \hat{\ } \rangle$, and the mean over several tidal cycles as $\overline{\ } \rangle$. The long term equilibrium flux through a given cross section is given by:

$$\widehat{us} = \widehat{u}_M \widehat{s}_M + \widehat{u'_M s'_M} + \overline{\widehat{u}_T \widehat{s}_T} + \overline{\widehat{u'_T (s'_M + s'_T)}} + \langle u's' \rangle_E \approx 0 \quad (1.4)$$

where u'_M, s'_M, u'_T, s'_T are deviations from their respective cross sectional means, $\widehat{u}_M, \widehat{s}_M, \widehat{u}_T, \widehat{s}_T$.

Defining flow into the estuary as positive, the first term on the right side is always negative and is the contribution of the net outflow of fresh water, \hat{u}_M being the cross sectional average of the tidally averaged flow. In the second term, gravitational circulation results in a positive deviation of the non-tidal flow, u_M' , near the bottom of the channel, and a negative u_M' near the surface. This vertical variation of the horizontal flow, when coupled with an increase of salinity with depth, contributes a net positive flux. The third term is the correlation of the cross sectional means of the tidal components, \hat{u}_T and \hat{s}_T . Within the salinity intrusion portion of estuaries with predominantly progressive wave tides, \hat{u}_T and \hat{s}_T are nearly out of phase, so that this term may not contribute significantly to the salt balance. The fourth term is the dispersion effect from vertical and lateral variation of the tidal current and provides the major salt intrusion mechanism in well mixed regions. The last term is the time and cross sectional average of the purely turbulent contribution to the salt flux. It is considered to be insignificant compared to the second and fourth terms.

A. Dispersion versus Diffusion

Turbulent diffusion as defined in this paper refers to the fluxes, $\langle u'w' \rangle_E$, $\langle u's' \rangle_E$, $\langle v's' \rangle_E$, $\langle w's' \rangle_E$, etc., that result from the smoothing of the equations of motion and salt conservation sufficient to make all variables deterministic. These turbulent fluxes must be parameterized as functions of the remaining deterministic variables.

The notion of dispersion, on the other hand, results when a further averaging of the equations is carried out over space and time scales that suppress details of the interaction among the deterministic variables as

they vary within the averaging interval.

The original reference on a dispersion mechanism is Taylor's classic model for pipe flow (Taylor, 1954). Oceanographic applications have been considered by Bowden (1965), Okubo (1967), and Kullenberg (1972). Taylor reasoned as follows: A vertical shear of a horizontal current near a boundary will advect differentially contaminants or hydrodynamic tracers. This advection spreads the tracer in the horizontal direction and weak vertical turbulent diffusion mixes the tracer in the vertical, producing an effective horizontal dispersion of the tracer much larger than the cross sectionally averaged horizontal turbulent diffusion. Vertically integrated models must parameterize this dispersion effect as well as that of turbulent diffusion. Taylor shows that horizontal dispersion is inversely proportional to the intensity of turbulent mixing. The results of Taylor and others suggests that if the detail with which the velocity field can be specified is increased, the necessity of specifying parameters that contain the effects of many physical processes involved in dispersion is reduced.

The last term in Equation (1.4) , $\overline{\langle u's \rangle}_E$, represents the diffusive flux, while the second and fourth terms are dispersion terms arising from cross sectional averaging. It is seen that the mean freshwater velocity, \hat{u}_M , is the only remaining deterministic horizontal velocity in a cross sectional and tidally averaged model. There is thus a trade-off between simplifying a model by depth and width averaging and the added necessity of parameterizing many physical processes involved in dispersion in terms of the few remaining variables.

B. The Basis of the Proposed Model and Review of Previous Work

In the present work a model of the effect of the gravitational circulation on salt intrusion in partially mixed estuaries is presented. The basic premise is that the extent of intrusion is best modelled by direct computation of the vertical variation of the horizontal velocities induced by the gravitational circulation. In this manner, the upstream flux of salt is computed directly, avoiding the necessity of parameterizing the effect of the gravitational circulation with a dispersion coefficient. The motion and salinity fields are strongly coupled because the magnitudes and vertical variation of the mean horizontal velocities influence the upstream flux of salt through the effect of vertical shear, and the salinity gradient determines horizontal accelerations.

In a recent paper, Fisher, Ditmars, and Ippen (1972) proposed a model to determine the longitudinal and vertical distributions of velocities and salinities in estuaries. They decouple the system by first establishing the horizontal variation of salinity with a one-dimensional salt equation, and then substitute this variation into the two-dimensional equations to find the vertical profile of mean horizontal velocities. Their approach necessitates an eddy dispersion coefficient in the one-dimensional model that already includes the effects of gravitational circulation on the upstream salt flux; thus, they have not solved the full two-dimensional problem. Their overall approach, however, has laid the groundwork for further developments of more sophisticated models of actual estuaries.

The classical papers on gravitational circulation were written by Rattray and Hansen (1962), Hansen (1967) and Hansen and Rattray (1965).

In the first paper the horizontal salinity variation is specified, formulating essentially the same type of model as proposed by Fisher et al. In the other two papers, a horizontal eddy diffusion term is defined, but not interpreted, which probably can be thought of as parameterization of the tidal dispersion terms in Equation (1.4). One method of solution is a series expansion in terms of the inverse of a mixing parameter proportional to their horizontal eddy coefficient. This has the effect of decoupling the system to the extent that the horizontal salinity gradient is determined solely by the tidal components of the salt flux without the gravitational component. A similarity solution is also found for the central regions of an estuary under several restrictive conditions. A solution, however, is obtained for the ratio of the gravitational component of the salt flux to the total upstream salt flux. While their work is the only definitive work on the problem, their methods of solution leave little room for refinement of their model to include detailed variations in specific estuaries; indeed that was not their purpose.

The following model, developed with the aid of numerical techniques, is a first step in the development of an estuarine circulation model which includes explicitly the physics of the gravitational circulation, and which can estimate the extent of salt intrusion. It is accessible to further refinement and specialization for use in specific estuaries. By specifying the vertical variation of the mean horizontal velocity throughout the estuary, the dispersion of a pollutant resulting from the vertical shear associated with the gravitational circulation can be calculated directly.

II. MATHEMATICAL FORMULATION

A. Governing Equations

Quantitative derivation is based upon conservation principles for water, salt and momentum. A right hand coordinate system is utilized with z positive upward and x positive into the estuary, and with the origin at mean sea level at an arbitrary seaward limit of the estuary as shown in Figure 1. The center of the channel or "Thalweg" is specified by $y = 0$. A Boussinesq hypothesis is used which specifies that variations of density are dynamically important only in determining the vertical pressure gradient. The major dynamic simplification is that the channel is specified as narrow; this restricts the cross channel velocity and renders Coriolis accelerations of secondary importance. The governing equations, which have been averaged over the ensemble so that all variables are deterministic, are

$$\frac{\partial \tilde{u}}{\partial t} + \frac{\partial \tilde{u}^2}{\partial x} + \frac{\partial \tilde{u}\tilde{v}}{\partial y} + \frac{\partial \tilde{u}\tilde{w}}{\partial z} - f\tilde{v} = -\frac{1}{\rho_0} \frac{\partial \tilde{p}}{\partial x} - \frac{\partial}{\partial x} \langle u'u' \rangle_E - \frac{\partial}{\partial y} \langle u'v' \rangle_E - \frac{\partial}{\partial z} \langle u'w' \rangle_E \quad (2.1)$$

$$\frac{\partial \tilde{v}}{\partial t} + \frac{\partial \tilde{u}\tilde{v}}{\partial x} + \frac{\partial \tilde{v}^2}{\partial y} + \frac{\partial \tilde{v}\tilde{w}}{\partial z} + f\tilde{u} = -\frac{1}{\rho_0} \frac{\partial \tilde{p}}{\partial y} - \frac{\partial}{\partial x} \langle u'v' \rangle_E - \frac{\partial}{\partial y} \langle v'v' \rangle_E - \frac{\partial}{\partial z} \langle v'w' \rangle_E \quad (2.2)$$

$$\frac{\partial \tilde{p}}{\partial z} = -g(\rho_0 + \delta\rho) \quad (2.3)$$

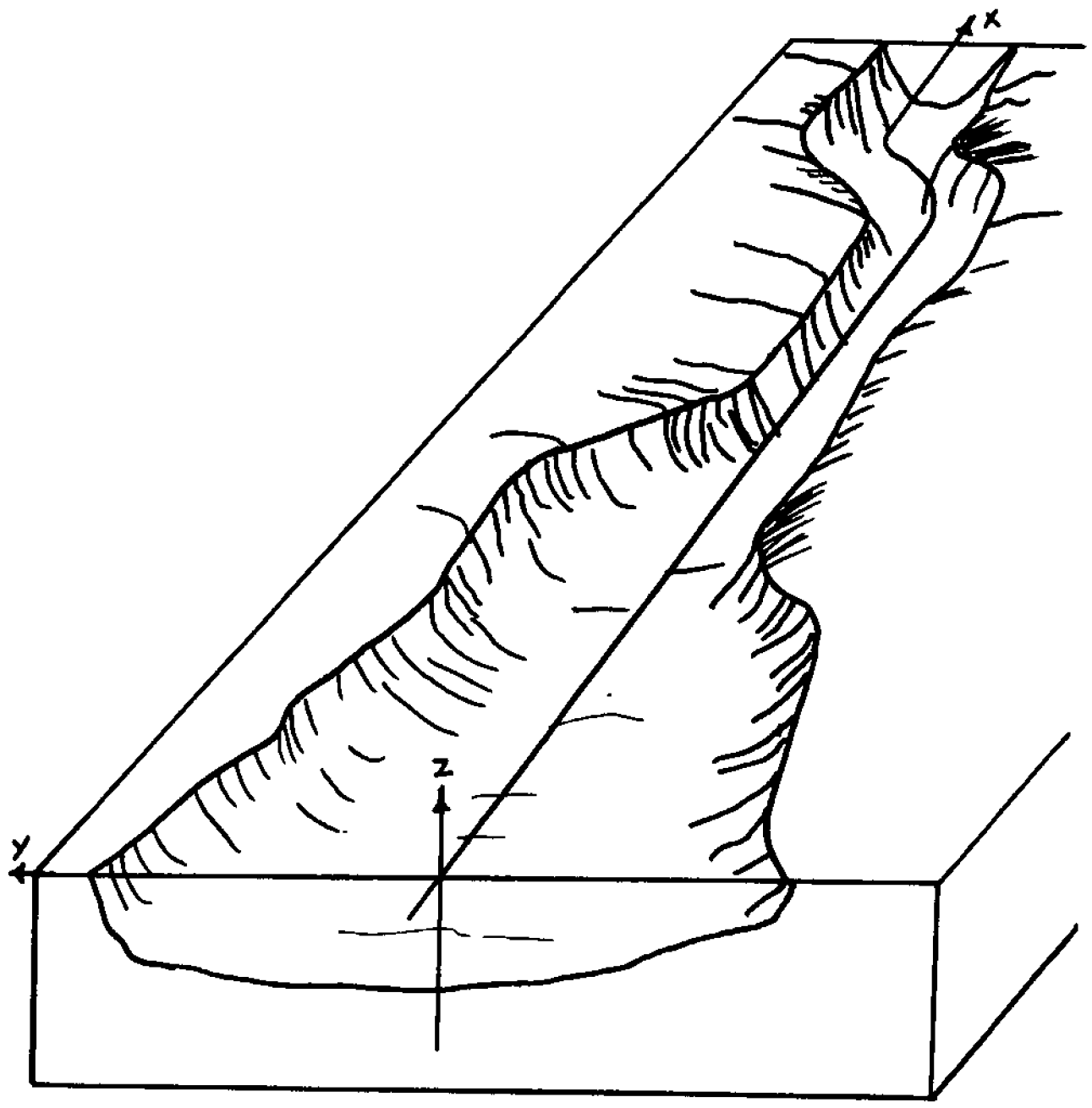


Figure 1. Specification of coordinate system

$$\frac{\partial \tilde{u}}{\partial x} + \frac{\partial \tilde{v}}{\partial y} + \frac{\partial \tilde{w}}{\partial z} = 0 \quad (2.4)$$

$$\frac{\partial \tilde{s}}{\partial t} + \frac{\partial \tilde{u}\tilde{s}}{\partial x} + \frac{\partial \tilde{v}\tilde{s}}{\partial y} + \frac{\partial \tilde{w}\tilde{s}}{\partial z} = - \frac{\partial}{\partial x} \langle u's' \rangle_E - \frac{\partial}{\partial y} \langle v's' \rangle_E - \frac{\partial}{\partial z} \langle w's' \rangle_E \quad (2.5)$$

The operators, $(\tilde{\quad})$ and $\langle \quad \rangle_E$, imply ensemble average.

The x, y, z components of velocity are \tilde{u} , \tilde{v} , \tilde{w} respectively. The salinity is specified as \tilde{s} and $\delta\rho$ is the deviation from the reference density ρ_0 . All prime quantities are turbulent fluctuations. The acceleration of gravity is g, P is pressure and f is the Coriolis parameter.

With the assumption that the dependence of density on temperature can be neglected compared to the density differences resulting from the extreme variations of salinity encountered in estuaries, an approximate equation of state is given by

$$\delta\rho = \beta (\tilde{s} - s_0)$$

with

$$\beta \equiv \frac{\partial \rho}{\partial s} \quad (2.6)$$

where s_0 is a reference salinity and β is an expansion coefficient.

Since cross-channel variations are considered of secondary importance for gravitational circulation, the equations are averaged over width. The variables are separated into their width average and deviation as follows:

$$\tilde{u} = u_b + u'_b, \text{ etc.} \quad (2.7)$$

with

$$u_b = \langle \tilde{u} \rangle_b \equiv \frac{1}{b(x,z)} \int_{b_1}^{b_2} \tilde{u} \, dy \quad (2.8)$$

where u'_b is the deviation of horizontal velocity from its width average, u_b , defined by (2.8). Variables, b_1 , b_2 , are the coordinates of the banks, and b is the width.

Cross-channel integration gives

$$\begin{aligned} \frac{\partial b u_b}{\partial t} + \frac{\partial b u_b^2}{\partial x} + \frac{\partial b u_b w_b}{\partial z} = & -\frac{b}{\rho_0} \frac{\partial p_b}{\partial x} - \frac{\partial}{\partial x} \left[b \langle u'_b u'_b + \langle u' u' \rangle_E \rangle_b \right] \\ & - \frac{\partial}{\partial z} \left[b \langle u'_b w'_b + \langle u' w' \rangle_E \rangle_b \right] + \frac{\tau_{b_2 x} (\sec \theta_2)}{\rho_0} - \frac{\tau_{b_1 x} (\sec \theta_1)}{\rho_0} \end{aligned} \quad (2.9)$$

$$f b u_b = -\frac{\tilde{p}(b_2)}{\rho_0} + \frac{\tilde{p}(b_1)}{\rho_0} - \frac{\partial}{\partial z} \left[b \langle \langle v' w' \rangle_E \rangle_b \right] \quad (2.10)$$

$$\frac{\partial (b u_b)}{\partial x} + \frac{\partial (b w_b)}{\partial z} = 0 \quad (2.11)$$

$$\begin{aligned} \frac{\partial b s_b}{\partial t} + \frac{\partial}{\partial x} (b u_b s_b) + \frac{\partial}{\partial z} (b w_b s_b) = & -\frac{\partial}{\partial x} \left[b \langle u'_b s'_b + \langle u' s' \rangle_E \rangle_b \right] \\ & - \frac{\partial}{\partial z} \left[b \langle w'_b s'_b + \langle w' s' \rangle_E \rangle_b \right] \end{aligned} \quad (2.12)$$

where the salt flux through the sides is taken as zero, $\tau_{b_i x}$ is the stress of the bank and θ_i is the angle between normal to the bank and the y -axis. The y equation (2.10) represents a balance between the cross-channel pressure gradient, friction, and the Coriolis term.

These equations are averaged over several tidal periods to analyze the transtidal flow.

The width averaged flow is separated into its tidal average and deviation as follows

$$u_b = \bar{u} + U_T, \text{ etc.} \quad (2.13)$$

with the tidal mean defined by

$$\bar{u} \equiv \frac{1}{nT} \int_{-nT/2}^{nT/2} u_b dt \quad (2.14)$$

The integrated equations become:

$$\begin{aligned} \frac{\partial}{\partial t} b\bar{u} + \frac{\partial}{\partial x} b\bar{u}^2 + \frac{\partial}{\partial z} b\bar{u}\bar{w} = & - \frac{b}{\rho_0} \frac{\partial \bar{p}}{\partial x} - \frac{\partial}{\partial x} \left[\langle bU_T^2 + b \langle u_b' u_b' + \langle u'u' \rangle_E \rangle_b \right] \\ & - \frac{\partial}{\partial z} \left[\langle bU_T W_T + b \langle u_b' w_b' + \langle u'w' \rangle_E \rangle_b \right]_T + \frac{\langle \tau_{b_2 x} \rangle_T (\sec \theta_2)}{\rho_0} - \frac{\langle \tau_{b_1 x} \rangle_T (\sec \theta_1)}{\rho_0} \end{aligned} \quad (2.15)$$

$$\frac{\partial b\bar{u}}{\partial x} + \frac{\partial b\bar{w}}{\partial z} = 0 \quad (2.16)$$

$$\begin{aligned} \frac{\partial}{\partial t} b\bar{s} + \frac{\partial}{\partial x} b\bar{u}\bar{s} + \frac{\partial}{\partial z} b\bar{w}\bar{s} = & - \frac{\partial}{\partial x} \left[\langle bU_T S_T + b \langle u_b' s_b' + \langle u's' \rangle_E \rangle_b \right] \\ & - \frac{\partial}{\partial z} \left[\langle b W_T S_T + b \langle w_b' s_b' + \langle w's' \rangle_E \rangle_b \right]_T \end{aligned} \quad (2.17)$$

where all barred quantities, such as \bar{u} , are width and time averages.

The terms on the right side of the equals sign, such as

$$\langle bU_T S_T + b \langle u_b' s_b' + \langle u's' \rangle_E \rangle_b \rangle_T$$

are interpreted as follows: The first term is the correlation over a tidal cycle of the width averaged velocity and width averaged salinity.

The second term is the tidal average of the lateral dispersion effect arising from width averaging. The last term is the width and tidal average of the turbulent horizontal salt flux.

With the use of the hydrostatic assumption, the pressure term becomes

$$\frac{\partial \bar{P}}{\partial x} = \frac{\partial \bar{P}_a}{\partial x} + \rho_0 g \frac{\partial \bar{\eta}}{\partial x} + g \int_z^{\bar{\eta}} \frac{\partial \delta \bar{\rho}}{\partial x} dz \quad (2.18)$$

where \bar{P}_a is atmospheric pressure and $\bar{\eta}$ is tidal mean elevation of the free surface. The second term represents the slope contribution to the pressure field, due in part to the fresh water head which drives the river downstream. The final term represents the baroclinic component resulting from the salinity distribution.

B. Simplification of the General Equations

Simplification is based upon the characteristics of the particular estuary to be simulated. For application to narrow partially mixed regions of estuaries such as the Hudson River above New York Harbor, the following assumptions are made.

1. Tides in the salinity intrusion region are primarily progressive, implying that

$$\langle U_T W_T \rangle_T = 0$$

2. Since the depth to width ratio is 1:25 and since the side stress terms are weighted by the reciprocal of the width when compared to other terms, side stress will be ignored.

3. The tidal stress terms,

$$\frac{\partial}{\partial x} \langle \langle u_b' u_b' \rangle_b \rangle_T \quad \text{and} \quad \frac{\partial}{\partial z} \langle \langle u_b' w_b' \rangle_b \rangle_T$$

are considered small compared to the turbulent stress

$$\frac{\partial}{\partial z} \langle \langle \langle u' w' \rangle_E \rangle_b \rangle_T$$

4. It will be assumed that bottom friction dissipates fluid accelerations locally. This allows the field terms to be dropped from the momentum equation. This assumption appears justified based upon data from the James River (Pritchard, 1956).

5. Since U_T and S_T are essentially out of phase, take

$$\langle U_T S_T \rangle_T = 0$$

6. Horizontal turbulent salt flux makes a negligible contribution.

The set of equations now reduce to

$$\frac{\partial}{\partial t} b\bar{u} = -bg \frac{\partial \bar{\eta}}{\partial x} - \frac{bg}{\rho_0} \int_z^\eta \frac{\partial \delta \bar{\rho}}{\partial x} dz - \frac{\partial}{\partial x} \langle bU_T^2 \rangle_T + \frac{\partial}{\partial z} \left(bA \frac{\partial \bar{u}}{\partial z} \right) \quad (2.19)$$

$$\frac{\partial b\bar{u}}{\partial x} + \frac{\partial b\bar{w}}{\partial z} = 0 \quad (2.20)$$

$$\delta \bar{\rho} = \beta (\bar{s} - s_0) \quad (2.21)$$

$$\frac{\partial}{\partial t} bs + \frac{\partial}{\partial x} bus + \frac{\partial}{\partial z} bws = - \frac{\partial}{\partial x} \langle b \langle u_b' s_b' \rangle_b \rangle_T + \frac{\partial}{\partial z} \left(bK_z \frac{\partial \bar{s}}{\partial z} \right) \quad (2.22)$$

where turbulent stress and turbulent salt flux have been parameterized by an eddy viscosity, A , and an eddy diffusivity, K_z , respectively.

For development purposes, a restrictive assumption will assume that the convective mode of salt intrusion predominates in the partially mixed

region. Under this assumption, the narrowness of the channel minimizes the dispersion effect of tidal shears on the salt transport. The first term on the right side of Equation (2.22) therefore will be dropped. The tides are interpreted as simply displacing the entire salt field upstream and downstream within the estuary. Bowden and Gilligan (1971) have demonstrated recently, in a region of the Mersey Estuary which is similar in many respects to the partially mixed region of the Hudson River, that the convective mode accounts for more than 75% of the upstream transfer of salt. A discussion of the relaxation of this assumption is given in the conclusion.

C. Final Formulation

Two-dimensionality of the continuity equation (2.20) allows definition of a transport stream function

$$b\bar{u} \equiv \frac{\partial \Psi}{\partial z}, \quad -b\bar{w} \equiv \frac{\partial \Psi}{\partial x} \quad (2.23)$$

By taking a z-derivative of the momentum equation (2.21), using $b\bar{b}(z)$, $U_T \neq U_T(z)$, and using the equation of state, derive a vorticity equation

$$\frac{\partial \xi}{\partial t} = -\frac{bg\beta}{\rho_0} \frac{\partial \bar{s}}{\partial x} + \frac{\partial^2}{\partial z^2} A \xi \quad (2.24)$$

where the vorticity is defined by

$$\xi = \frac{\partial b\bar{u}}{\partial z} = \frac{\partial^2 \Psi}{\partial z^2} \quad (2.25)$$

The salt equation becomes

$$\frac{\partial b\bar{s}}{\partial t} = \frac{\partial}{\partial x} b\bar{u}\bar{s} + \frac{\partial}{\partial z} b\bar{w}\bar{s} = \frac{\partial}{\partial z} \left(bK_z \frac{\partial \bar{s}}{\partial z} \right) \quad (2.26)$$

D. Boundary Conditions

The surface boundary conditions are assumed to apply at $z = 0$. Wind stress at the surface is given by

$$-\langle \langle \langle \frac{\tau_w}{\rho} \rangle_E \rangle_b \rangle_T = \langle \langle \langle u'w' \rangle \rangle \rangle_{E b T} \quad z = 0 \quad (2.27)$$

Flux of water across this boundary is equivalent to the tributary inflow per unit length, R , from tributaries and free run-off

$$\frac{\partial \Psi}{\partial x} = R \quad z = 0 \quad (2.28)$$

At the bottom no slip and no flow through the bottom are specified.

$$\begin{aligned} \frac{\partial \Psi}{\partial z} &= 0 & z &= -h(x) \\ \Psi &= 0 & z &= -h(x) \end{aligned} \quad (2.29)$$

The conditions on salt specify no loss of salt through either the surface or bottom boundary

$$\langle \langle \langle w's' \rangle_E \rangle_b \rangle_T + \bar{w}\bar{s} = 0 \quad z = 0 \quad (2.30)$$

$$\langle \langle \langle w's' \rangle_E \rangle_b \rangle_T = 0 \quad z = -h(x) \quad (2.31)$$

The formulation using vorticity and stream function eliminates the specification of the barotropic component of the pressure field. This condition is replaced by the necessity of specifying the net river flow through all cross-channel cross sections by the difference in the values of the stream function between the surface and bottom boundaries.

A tidally averaged vertical salinity profile is specified at the seaward boundary and fresh water is assumed at the upstream boundary. The model must have a large enough horizontal extent so that salinity reaches

zero well before the upstream boundary; this is to insure that the upstream boundary does not force the solution in the region of interest.

E. Turbulent Processes

Estuarine studies are plagued by the importance of turbulent processes. Geophysical turbulent processes in stratified fluids have been and still are not well understood. Parameterization of expected values of turbulent fluxes as functions of deterministic variables is understood even less. Stratified fluids in particular are subject to possible turbulence induced by breaking of internal waves. Estimates of turbulent processes are not only necessary to determine vertical diffusion of salt, but also to determine the transfer of vorticity into the fluid from the no slip boundary.

Both previously mentioned gravitational circulation models assumed constant eddy coefficients. This had the effect of underestimating the velocities near the bottom (Hansen and Rattray, 1965, see figure 2). Since the velocity profile plays a critical role in advecting salt into the estuary, the vertical variation of turbulent processes will be shown to affect the limit of salt intrusion. These models were concerned primarily with matching vertical variations and were either incapable of estimating the effect of vertical eddy coefficients on horizontal salinity profiles or did not explore this aspect.

Turbulence parameterizations fall into three general categories.

1. Turbulent-viscosity concept: The stress term, $\tau = -\rho \overline{u'w'}$ is replaced by $A \frac{\partial \bar{u}}{\partial z}$, where the eddy viscosity is a property of the local state of turbulence and is to be further parameterized as either

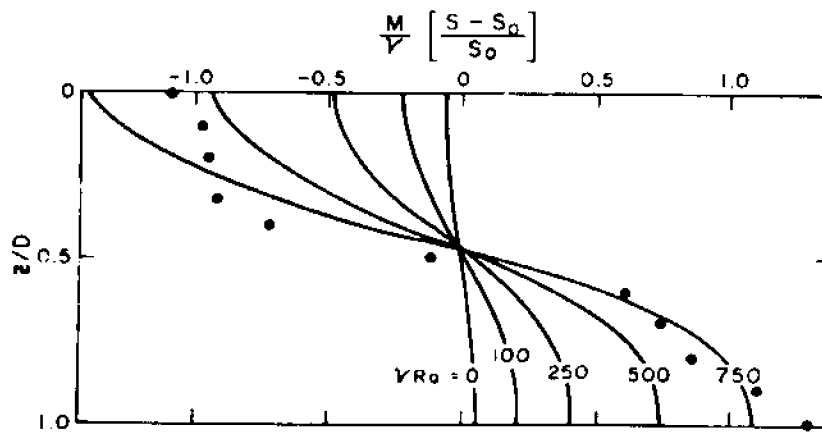
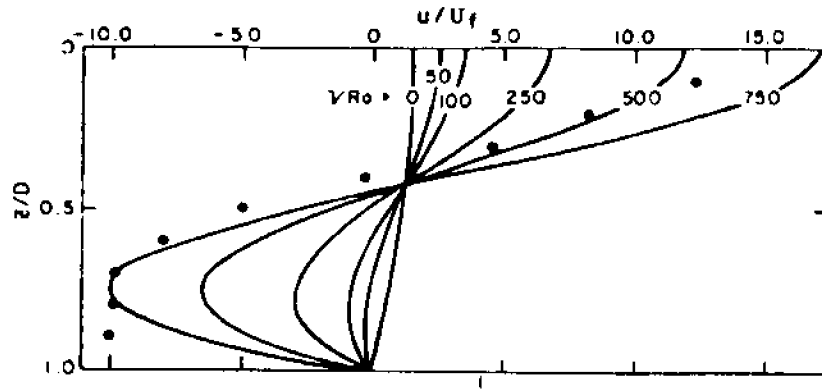


Figure 2. Solutions for constant eddy coefficient cases. Upper figure plots non-dimensional velocity vs. depth and lower figure plots non-dimensional salinity vs. depth as function of an estuary analogue of the Rayleigh number. Dots are James River data. (After Hansen and Rattray, 1965).

a fixed function of space, algebraically dependent on deterministic variables, or determined from its own differential equation of transport.

2. Stress transport model: where the stress is proportional to the turbulent energy, $\tau \propto k$, with $k^2 = u'^2 + v'^2 + w'^2$. A differential transport equation is written for k .

3. Differential stress model: A differential equation is written directly for the stress

$$\frac{D\tau}{Dt} = \dots$$

with the problem closed at higher order.

The state of the art in geophysical problems is to use the turbulent viscosity hypothesis, but special care should be taken near boundaries and where $\partial\bar{u} / \partial z \rightarrow 0$.

Eddy diffusivities, as well as eddy viscosities, can be considered dimensionally as the product of a characteristic velocity scale and a characteristic length scale

$$K \sim u^* \ell^* \tag{2.32}$$

Kent and Pritchard (1959) tested Prandtl's mixing hypothesis for balancing salt flux in the James River by using

$$K_z = \lambda^2 \ell^2 \left| \frac{\partial\bar{u}}{\partial z} \right| \tag{2.33}$$

with λ a constant and ℓ a mixing length. The velocity scale was related to the vertical gradient of mean velocity. For neutral stability (adiabatic mixing) the mixing length, ℓ , was taken as that for flow between parallel plates

$$\ell_a = \frac{\kappa z (H-z)}{H} \tag{2.34}$$

where H is the depth of the fluid, and κ is von Karman's constant.

This length was reduced for stratified conditions by parameterizing the mixing length further with a Richardson number dependence. Two of the dependences used were

$$\ell = \ell_a (1 + \mu R_i)^{-\frac{1}{2}} \quad (2.35)$$

and

$$\ell = \ell_a (1 + \gamma R_i)^{-1} \quad (2.36)$$

where μ and γ are unknown proportionality factors and R_i is the local Richardson number

$$R_i = \frac{\frac{g}{\rho_0} \frac{\partial \bar{\rho}}{\partial z}}{\left(\frac{\partial \bar{u}}{\partial z}\right)^2} \quad (2.37)$$

Agreement between observed mixing lengths calculated from extensive James River data and both theoretical models, (2.35) and (2.36), suggests that Kent and Pritchard's approach is reasonable. Improvement was obtained when the adiabatic mixing lengths above mid-depth were increased. Kent and Pritchard suggest that the improvement is due to inclusion of the effects of surface waves, but the cause may also be related to having a free slip condition on the upper surface rather than a rigid plate assumed in (2.34).

Pritchard (1960) reasoned that the velocity scale in (2.32) should be related more correctly to the average speed of the entire current, including both the mean and tidal components. With the length scale taken to be the mixing length, ℓ , his vertical eddy coefficient, neglecting wind effects, becomes

$$K_z = \frac{\lambda U_a z^2 (H-z)^2}{H^3} (1 + \mu R_i)^{-2} \quad (2.38)$$

where U_a is the average speed of the current.

Since tidal velocities are an order of magnitude larger than the mean flow, most of the turbulent energy is derived from the tidal flow; thus the velocity in the Richardson number expression associated with turbulent energy production should be related more correctly to the average speed of the current rather than to the mean velocity.

$$\frac{\frac{g}{\rho_0} \frac{\partial \bar{\rho}}{\partial z}}{\langle \left| \frac{\partial U a}{\partial z} \right|^2 \rangle_T} \quad (2.39)$$

The eddy diffusivity, K_z , and eddy viscosity, A , are theoretically equal only under non-stratified conditions. Bowden (1967) and more recently Bowden and Gilligan (1971), discuss the ratio $K_z:A$ observed in the Mersey Estuary over a range of Richardson number as defined by (2.39). Bowden makes the interesting point that this curve is very close to that derived by Munk and Anderson (1948) in connection with a theory of the thermocline. They proposed the following empirical relations

$$A = A_0 (1 + 10 R_i)^{-1/2} \quad (2.40)$$

$$K_z = A_0 (1 + 3.33 R_i)^{-3/2} \quad (2.41)$$

where A_0 is the mixing coefficient for adiabatic conditions. This variation is plotted in Figure 3.

The following conclusions can now be stated.

1. Variable coefficients are necessary and should not be replaced by virtual constant coefficients.
2. These coefficients should be functions of depth but their exact algebraic form is uncertain especially near the surface.

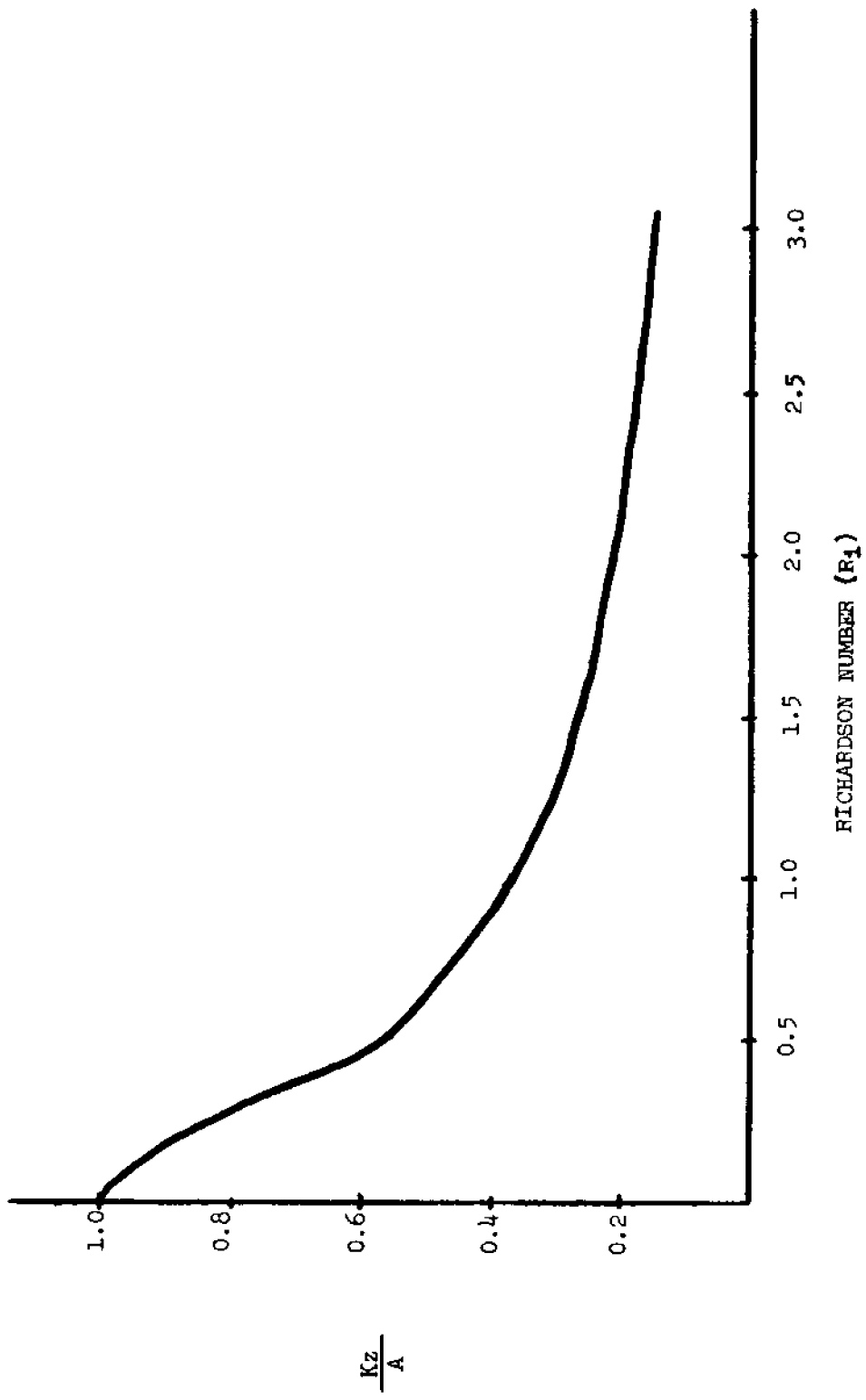


Figure 3. Dependence of the ratio of eddy diffusivity to eddy viscosity upon Richardson number as hypothesized by Munk and Anderson (1948) and verified for the Mersey Estuary by Bowden and Gilligan (1971).

3. Turbulent energy is predominantly derived from the tidal flow; thus the tidally averaged Richardson numbers are functions of stability but are not primarily related to the mean velocity profiles, $\partial\bar{u}/\partial z$.

4. Allowance should be made for the separate variations of eddy diffusivity and viscosity as functions of Richardson number.

Observed and theoretically assumed values for eddy coefficients for tidally averaged flow in partially mixed estuaries are presented in Table 1.

Since many different assumptions about mixing effects can be plausibly made because of the lack of knowledge of the dependence of the eddy coefficients upon depth, tidal velocities and stability, no definitive formulation is possible. The above conclusions, however, suggest the important types of variations that should be included.

For non-constant coefficient cases, the model will use an assumed vertical variation of the eddy coefficients for neutral conditions as graphed in Figure 4. The coefficient for the adiabatic condition is labeled $KM(z)$, with a maximum, KM . The values on the surface and bottom, $J = 1$, $J = B$, are special since they are related to transfer processes across the boundaries of the fluid, as opposed to redistribution within the fluid.

Dependence on stratification is based upon the formulation of the Richardson number given by (2.39) and upon Munk and Anderson's equations (2.40) and (2.41). The denominator of the Richardson number (2.39) was estimated following Pritchard (1960)

$$\left| \left(\frac{.7 U_{am}}{H} \right)^2 \right| \tag{2.42}$$

Table I. Assumed and observed values for vertical eddy coefficients of previous investigators. Values correspond to tidally averaged flow.

| INVESTIGATORS | K_z (cm^2/sec) | A (cm^2/sec) | LOCATION |
|--|---------------------------------------|-----------------------------------|------------------|
| <u>Theoretically assumed constant coefficients</u> | | | |
| Rattray and Hansen (1962) | 2 | 4 | James River |
| Fisher et al. (1972) | .16 | .22 | Flume |
| | 1.6-5 | 4.5-12 | James River |
| Hansen and Rattray (1972) | 0.5 | 5 | Baltimore Harbor |
| <u>Calculated from data</u> | | | |
| Pritchard (1960) | | | |
| Maximum value in vertical profile | 6.5 | - - | James River |
| Minimum " " " " | 1.0 | - - | James River |
| Bowden (1965) | | | |
| Maximum value in vertical profile | 32 | - - | Mersey Estuary |
| Minimum " " " " | 6 | - - | Mersey Estuary |
| Bowden and Sharaf El Din (1966) | | | |
| Maximum value in vertical profile | 17-28 | 29 | Mersey Estuary |
| Minimum " " " " | 1-3 | 8.5 | Mersey Estuary |

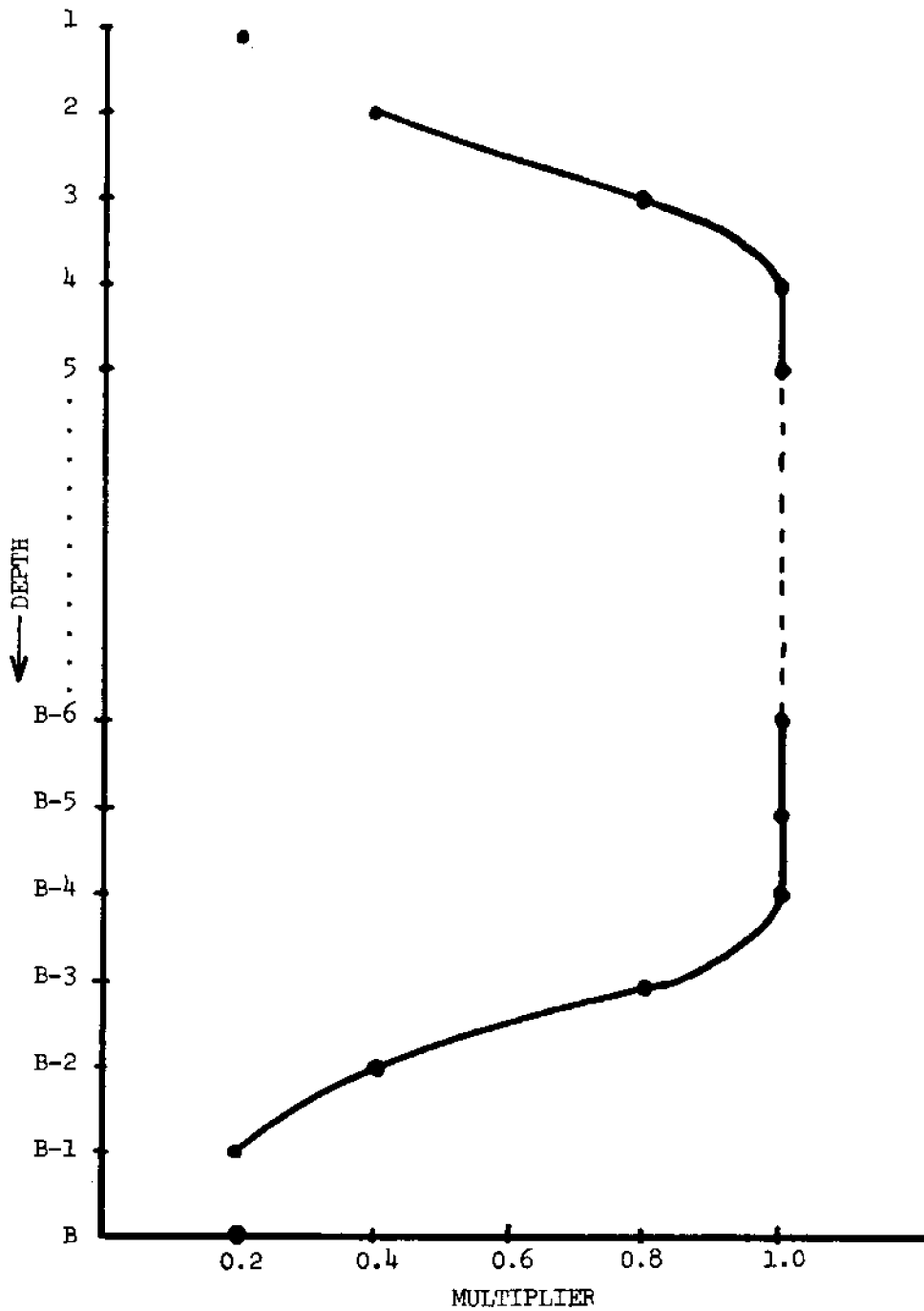


Figure 4. Assumed vertical variation of eddy coefficients for neutral conditions.

where U_{am} is the maximum speed at mid-depth. A value of 1 m/sec was assumed for U_{am} throughout the length of the model. At all interior points $2 \text{ cm}^2/\text{sec}$ is added to all values to provide an absolute minimum value for the coefficients. In summary, it was assumed that the adiabatic eddy coefficients are modified by stability as follows:

$$A = 2 + KM(z) [1 + 3.3 \Delta s]^{-1/2} \quad (2.43)$$

$$K_z = 2 + KM(z) [1 + \Delta s]^{-3/2} \quad (2.44)$$

where Δs is the difference in the value of salinity at adjacent grid points one meter apart, and K_z and A are given in units of cm^2/sec .

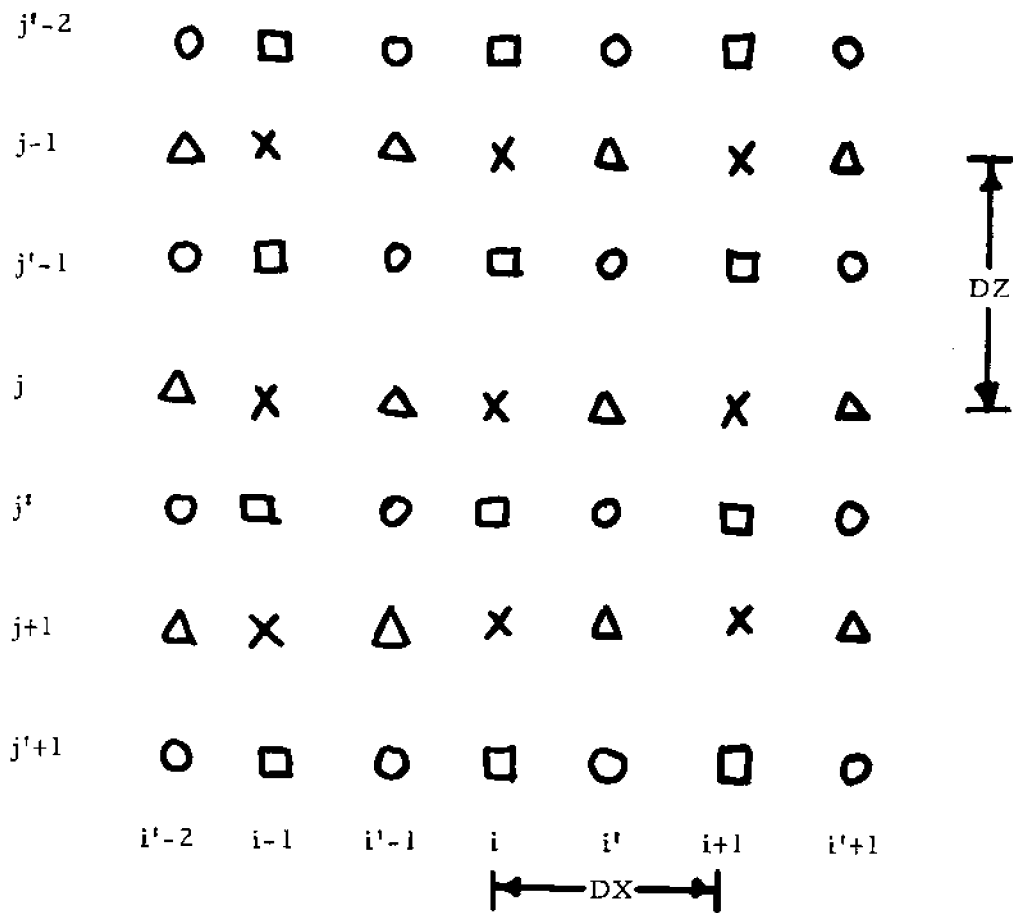
In the event that unstable stratification should develop during the computations, complete vertical mixing of the unstable water is assumed. This is accomplished by setting the eddy coefficients above the unstable layer at an effective infinity $0(10^6)$ for one iteration when an unstable situation develops. This procedure is similar to the method used by Bryan (1969).

III. METHOD OF SOLUTION

"If the time-step were 3 hours, then 32 individuals could just compute two points so as to keep pace with the weather"

L. F. Richardson, 1921

The coupled salt and momentum equations are solved numerically on a staggered grid as shown in Figure 5. Stream function and vorticity points intersect the top and bottom boundaries with the value of the stream function prescribed on both boundaries, the vorticity on the



LOCATION

X
○
◻
△

PARAMETERS DEFINED AT THIS LOCATION

Salt

Vorticity, Streamfunction, Vertical Eddy Viscosity

W-Transport, Vertical Eddy Diffusivity

U-Transport

Figure 5. Specification of numerical grid.

free surface prescribed from the wind stress

$$\langle b \langle \langle \frac{\tau}{\rho_0} \rangle_E \rangle_b \rangle_T = A \xi_0 \quad (3.1)$$

and vorticity on the lower boundary estimated by

$$\xi_N = \frac{2 (\psi_n - \psi_{n-1})}{(\Delta z)^2} \quad (3.2)$$

in a manner similar to Bryan (1963).

The salinity points are offset from the stream function and vorticity points in such a manner that salt points lie in the center of an array of four stream function points. These four points form a cell or box, and volume transport across any surface of the box is estimated by differencing adjacent stream function points.

The coupled salt and vorticity equations have the form of time dependent advection-diffusion equations similar to the set used in Bénard cell problems. A general approach to solving the Bénard problem numerically has been central differencing of time derivatives used in conjunction with a Jacobian of the type suggested by Arakawa (1966) that maintains certain integral constraints on the flow, such as conservation of scalar quantities. For the diffusion terms in the equations, several researchers have chosen the numerically stable DuFort-Frankel operator. However, it has recently been shown (Overland, 1973) that this diffusion operator is not necessarily conservative of scalar variables.

An alternative discretization which does not require a prohibitively small time step is the following implicit scheme that requires simultaneous solution for all points in a vertical column. The scheme

chosen is attributed to Laasonen (1949). The advection terms have the standard leapfrog formulation.

$$S_{ij}^{t+1} - S_{ij}^{t-1} = \frac{2\Delta t}{b_i} \cdot JS_{ij}^t + \frac{2\Delta t}{(\Delta z)^2} \cdot \quad (3.3)$$

$$\left[KZ_{ij+\frac{1}{2}} S_{ij+1}^{t+1} - KZ_{ij+\frac{1}{2}} S_{ij}^{t+1} - KZ_{ij-\frac{1}{2}} S_{ij}^{t+1} + KZ_{ij-\frac{1}{2}} S_{ij-1}^{t+1} \right]$$

where the Jacobian, JS_{ij}^t is defined by

$$JS_{ij}^t = \frac{1}{2\Delta x \Delta z} \left[\left(\Psi_{i-1, j-1} - \Psi_{i-1, j} \right) \left(S_{i-1, j} + S_{ij} \right) \right. \\ \left. - \left(\Psi_{ij-1} - \Psi_{ij} \right) \left(S_{ij} + S_{i+1, j} \right) - \left(\Psi_{ij} - \Psi_{i-1, j} \right) \left(S_{ij} + S_{ij+1} \right) \right. \\ \left. + \left(\Psi_{ij-1} - \Psi_{i-1, j-1} \right) \left(S_{ij-1} + S_{ij} \right) \right] \quad (3.4)$$

In a like manner the vorticity equation is

$$\xi_{ij}^{t+1} - \xi_{ij}^{t-1} = -b_i \frac{\Delta t \beta}{\Delta x} \left[\left(S_{i+1, j+1}^t + S_{i+1, j}^t \right) - \left(S_{ij+1}^t + S_{ij}^t \right) \right] \quad (3.5) \\ + \frac{2\Delta t}{(\Delta z)^2} \left[A_{ij+1} \xi_{ij+1}^{t+1} - A_{ij} \xi_{ij}^{t+1} - A_{ij} \xi_{ij}^{t+1} + A_{ij-1} \xi_{ij-1}^{t+1} \right]$$

The form of the advection term, JS_{ij} , conserves S and S^2 when summation is made over all interior grid points. The staggered grid insured no contribution to S or S^2 arising from either the surface or bottom boundaries.

The tri-diagonal nature of the matrix allows solution of this system directly by a Gaussian elimination scheme given in Richtmyer and Morton (1967).

The general sequence of operations for one time step is as follows:

1. Solve the salinity equation with time step Δt .
2. Solve the vorticity equation with time step Δt .
3. Solve for the stream function from the vorticity field using $\frac{\partial^2 \Psi}{\partial z^2} = \xi$. This is accomplished by solving the vector equation

$$[M] \underline{\Psi} = \underline{\xi} \quad (3.13)$$

where $B_j = 2$ and A_j and $C_j = -1$.

4. Determine the new bottom boundary conditions on ξ from equation (3.2) and specify the new wind stress, runoff and eddy coefficients.
5. Go to 1.

A forward time step was substituted every 20 iterations to control the weak divergence of the numerical solutions at adjacent time levels that is inherent in central time differencing.

Inspection of the salt balance equation (3.3) reveals no smoothing of the salinity field in the x-direction. This is due to the hypothesis that the major salt balance is between horizontal advection and vertical diffusion and advection. The lack of smoothing permits the growth of spurious computational modes to go unchecked and could allow anomalously large gradients to develop that could destroy the numerical computations. In the estuary, horizontal diffusion and dispersion processes control

extreme gradients, even though they play a small part in the total salt balance. These effects could be included by the addition of a horizontal dispersion term parameterized by a horizontal eddy coefficient. However, this term would add dispersive salt flux and the intra-tidal dispersion effects may bear little relation to tidal mean variables. It was decided that these effects could be represented more realistically by a conservative smoothing-desmoothing operator applied in the x-direction after each iteration (Haltner, 1971, p. 270). The operator has the form:

$$\begin{aligned}\tilde{f}_i &= \frac{1}{4} (f_{j+1} + 2f_i + f_{i-1}) \\ \bar{f}_i &= \frac{1}{4} (-\bar{f}_{j+1} + 6\bar{f}_i - \bar{f}_{i-1})\end{aligned}\tag{3.14}$$

This operator can be considered a low pass filter which removes two grid length oscillations, considered as noise in the numerical solution, but does not amplify wavelengths larger than $2 \Delta x$.

IV. RESULTS

A series of cases were investigated to determine the flexibility of the model and to determine its sensitivity to various assumptions regarding turbulent mixing. It is difficult to determine what comprises a typical estuary because detailed geometry, tidal velocities and stratification vary considerably, but the gross features of many partially mixed regions tend to have similar characteristics. The restrictions of the present model on horizontal tidal mixing, however, limit

discussion to relatively narrow stretches, excluding Chesapeake Bay and similar estuaries with wide gently sloping cross sections.

The data used for the model configuration are generalized from the Hudson River upstream from the lower tip of Manhattan Island. A constant depth of 14 meters, a constant width of 1040 m, and a constant run-off value of $212.4 \text{ m}^3/\text{sec}$ (7500 cubic feet/sec (cfs)) were assumed. This value for run-off is representative of an intermediate discharge rate. An observed vertical salinity profile was maintained at the mouth end.

A vertical resolution of one meter was picked for the value of DZ , giving 14 layers in the vertical. A horizontal grid length of 6 kilometers was assigned. Although 6 km would be too large a distance to resolve bathymetry adequately in a variable depth model, it was felt that computer resources would be utilized best by running more cases on a coarse mesh. The model nominally has twenty-six segments in the horizontal, which correspond to a distance of about 150 km from the Battery at the lower tip of Manhattan to Poughkeepsie. In one case, the model was extended to fifty segments when the salt intruded past the twentieth segment. The numerical time step was twenty minutes.

Thirteen cases were examined. Their assumptions are listed in Table II. The various parameters can be interpreted in the following manner: The salinity gradient and wind stress generate vorticity, accelerating the flow. These vorticity tendencies are countered by vorticity generation required by no slip on the bottom boundary. The vertical eddy viscosity, A , provides a measure of the rate with which

Table II. Tabulation of cases run

| Case | Constant coefficients | A cm ² /sec | KZ or RM cm ² /sec | Stability Dependent | ft ³ /sec | Run-off m ³ /sec | Wind | Figure Number |
|------|-----------------------|---------------------------|----------------------------------|------------------------|----------------------|--------------------------------|------|------------------|
| I | Yes | 4 | 4 | No | 7500 | 212.4 | No | 6 |
| II | Yes | 8 | 4 | No | 7500 | 212.4 | No | 7 |
| III | Yes | 10 | 10 | No | 7500 | 212.4 | No | 8 |
| IV | Yes | 25 | 25 | No | 7500 | 212.4 | No | 9 |
| V | No | -- | 10 | No | 7500 | 212.4 | No | 10 |
| VI | No | -- | 10 | Yes | 7500 | 212.4 | No | 12 |
| VII | No | -- | 15 | Yes | 7500 | 212.4 | No | 13 |
| VIII | No | -- | 20 | Yes | 7500 | 212.4 | No | 14 |
| IX | No | -- | 10 | Yes | 3500 | 99.1 | No | 16 |
| X | No | -- | 10 | Yes | 15000 | 424.8 | No | 17 |
| XI | No | -- | 15 | Yes | 5000 | 141.6 | No | 19 |
| XII | No | -- | 20 | Yes | 5000 | 141.6 | No | 20 |
| XIII | No | -- | 10 | Yes | 7500 | 212.4 | Yes | 22 |

boundary generated vorticity diffuses into the fluid. The intrusion of the density layer is countered by the net seaward flow of the river run-off. The salt balance is maintained by the vertical diffusion and advection of salt. The vertical diffusion is a function of the eddy diffusivity, K_z .

The first four cases test four different assumptions for vertical mixing with constant coefficients. These cases were run from the initial condition of no salt in the system to steady state values.

Case I (Figure 6) portrays the salinity, transport stream function, and horizontal velocities using a value for both eddy diffusivity and eddy viscosity coefficients of $4 \text{ cm}^2/\text{sec}$. The salinity field is given in parts per thousand and is contoured at 1, 5, 10, 15, and 20 ppt. The transport stream function is plotted in units of cm^3/sec times 10^{-8} . Contour lines are for values of -1, 2, 5, 8. The dashed line represents the transition from the freshwater contribution to the seawater contribution to the total volume flux. The volume transport between adjacent grid points is obtained by dividing the stream function difference by the grid length. The laterally averaged horizontal velocity component is given in units of cm/sec ; negative values represent seaward flow and positive values are landward flow. Isotachs are given at plus and minus 5, 10, 15, and 20 cm/sec .

The salinity increases with depth and decreases landward, and the horizontal velocity field shows a strong reversal with depth and absolute velocities of the right order of magnitude when compared to direct measurement in the James River and other estuaries. (To my knowledge, no data are available as to the vertical variation of the tidal mean flow for the Hudson

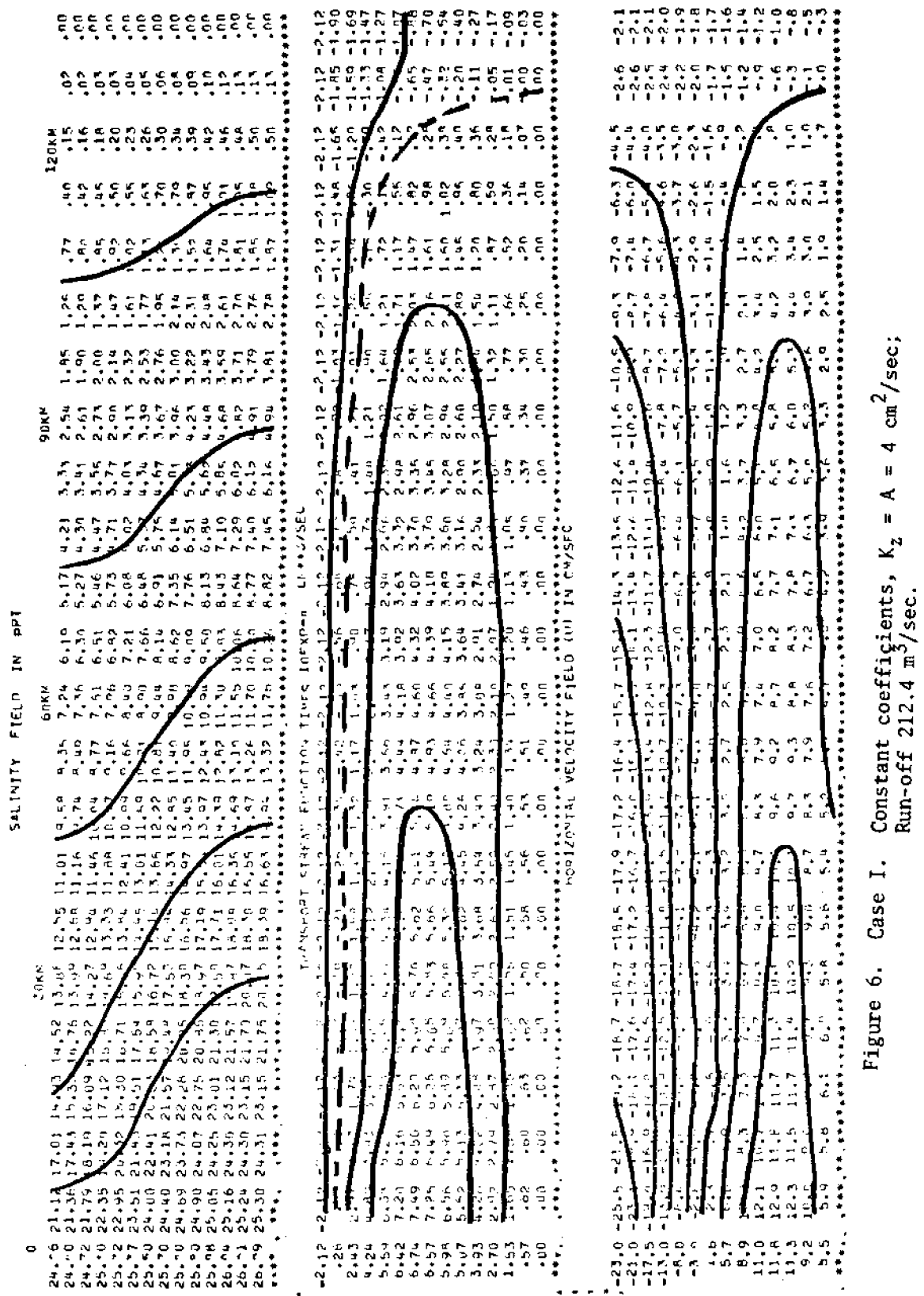


Figure 6. Case I. Constant coefficients, $K_2 = A = 4 \text{ cm}^2/\text{sec}$;
Run-off $212.4 \text{ m}^3/\text{sec}$.

River.) Note that the velocities associated with the gravitational circulation are much larger than those for the freshwater region at the extreme right of the figure. Vertical components of the transport stream function are indicative of vertical velocities. Vertical transport is necessary for conservation of volume flux, and it also furnishes an upwelling component to the salt balance. The reduction in velocities at the extreme seaward end is a result of smoothing the first interior salt point while maintaining the salinity values on the seaward boundary as fixed. The reduction of the gravitational circulation velocities at the seaward end is interpreted as being necessary for the transition to a vertically mixed circulation system beyond the seaward limit of the model, where density effects are diminished.

For small values of the eddy coefficients, salt intruded well into the model. This run may be contrasted with Case II shown in Figure 7 in which the assumption of strong stratification effects from large Richardson number was made. Unequal but constant values of $K_z = 4 \text{ cm}^2/\text{sec}$ and $A = 8 \text{ cm}^2/\text{sec}$ were used to specify the different values of eddy diffusivity and eddy viscosity in stratified conditions. This case corresponds to the type of eddy coefficient dependences used both by Rattray and Hansen (1962) and Fischer et al (1972). It is seen that, for equivalent run-off conditions, increasing the rate that boundary generated vorticity diffuses into the interior has a considerable effect upon the limit of intrusion.

In Case III (Figure 8) and Case IV (Figure 9), equal coefficients for viscosity and diffusivity again are assumed implying low Richardson number

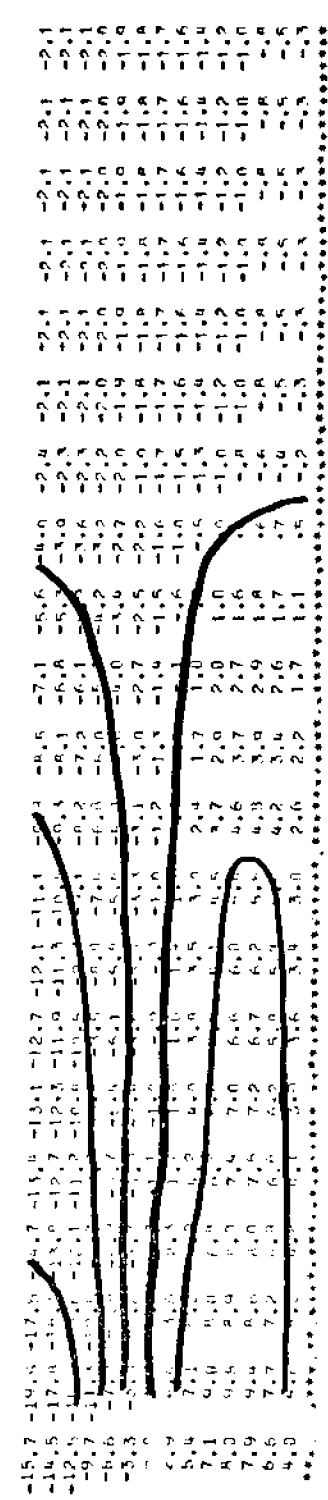
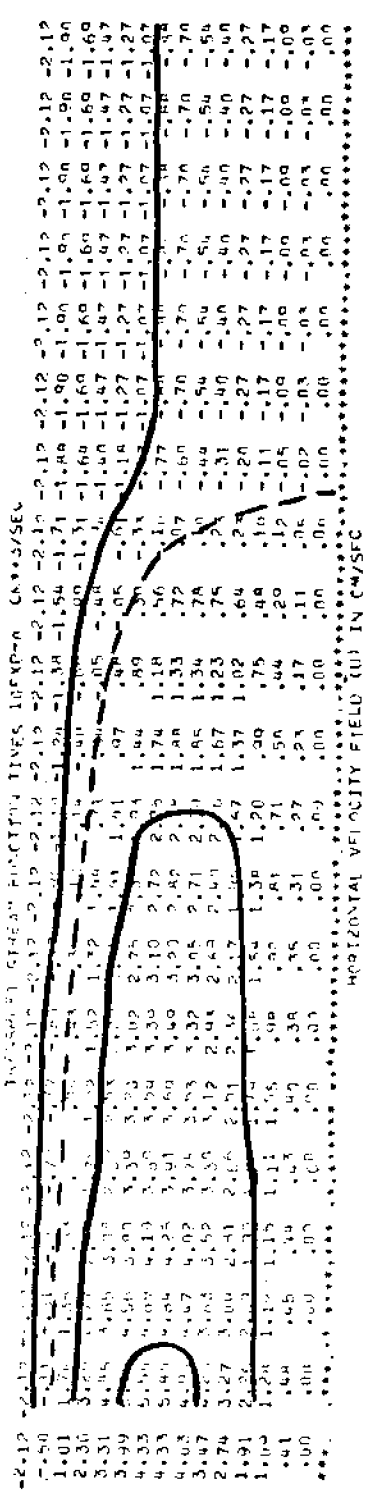
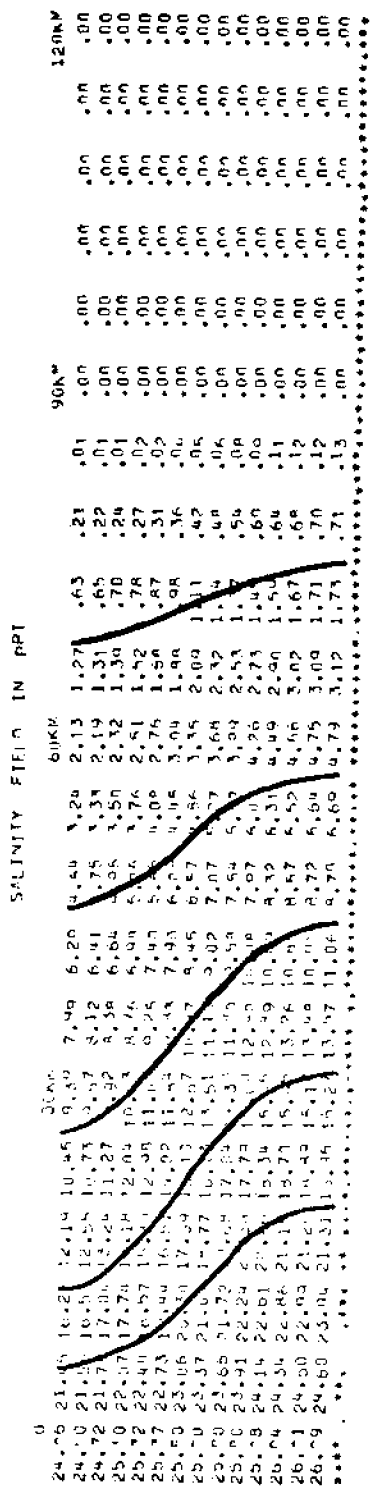


Figure 7. Case II. Constant coefficients, $K = 4 \text{ cm}^2/\text{sec}$;
 $A = 8 \text{ cm}^2/\text{sec}$; Run-off $\bar{Z}12.4 \text{ m}^3/\text{sec}$.

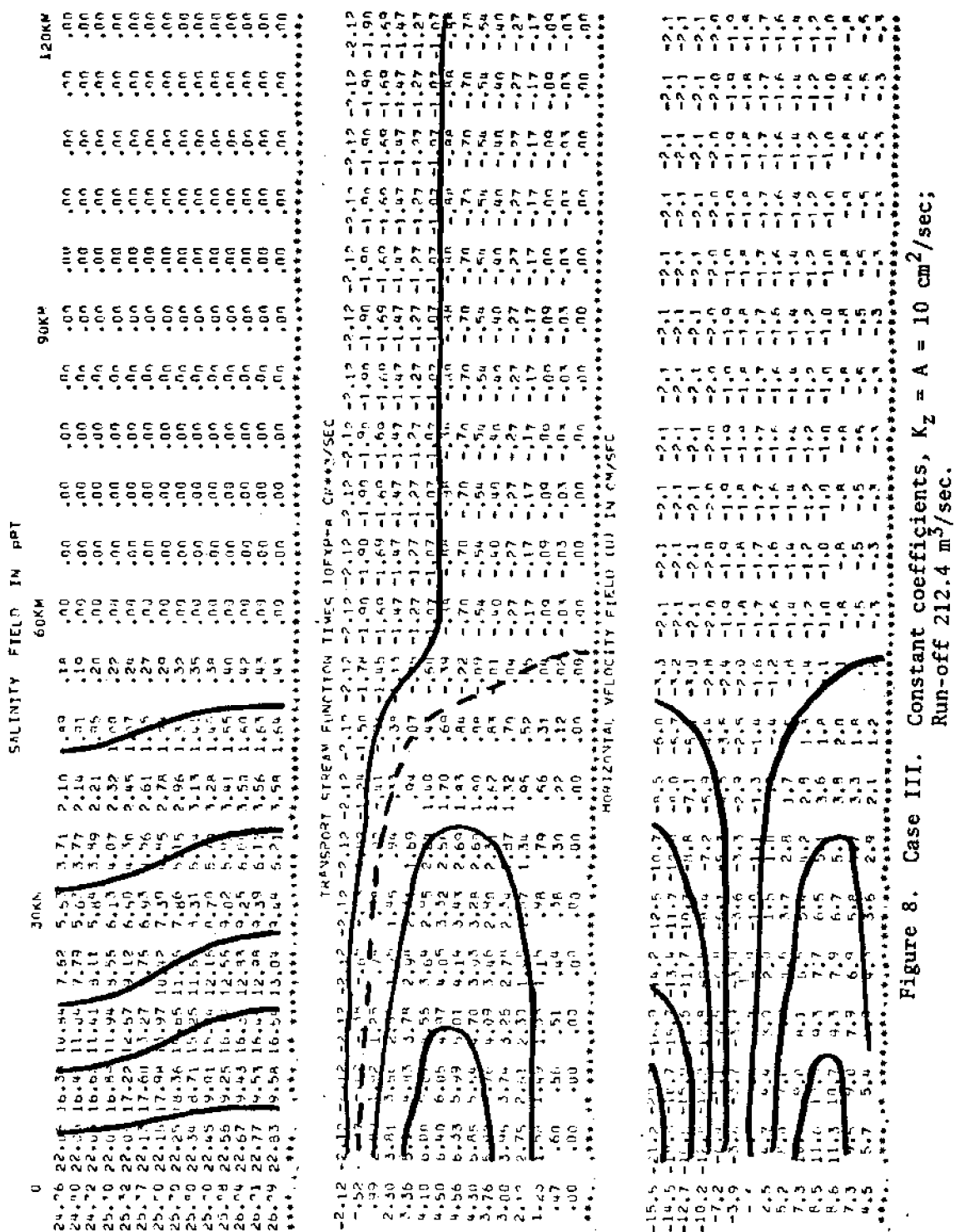


Figure 8. Case III. Constant coefficients, $K_z = A = 10 \text{ cm}^2/\text{sec}$;
Run-off 212.4 m^3/sec .

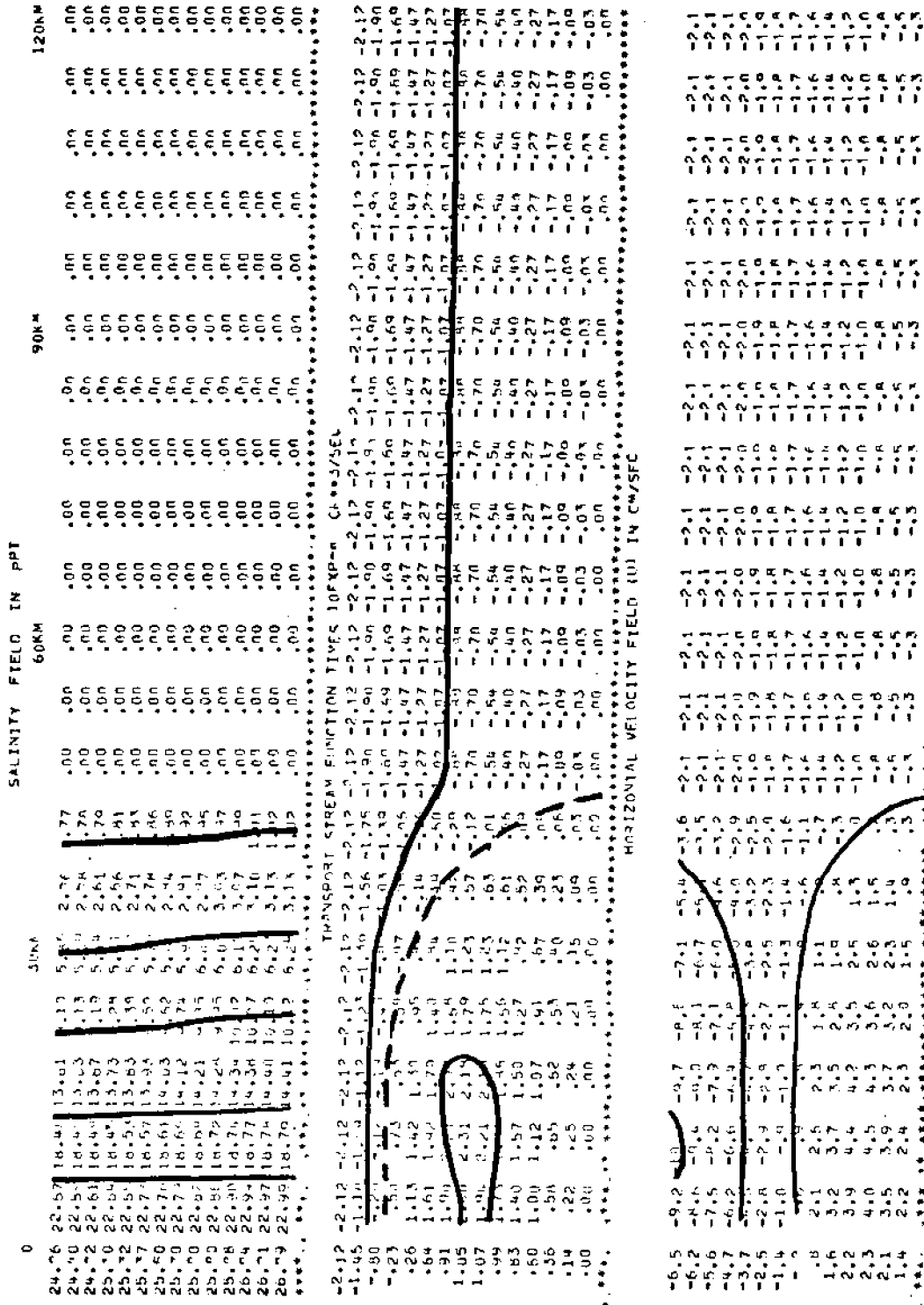


Figure 9. Case IV. Constant coefficients, $K_z = A = 25 \text{ cm}^2/\text{sec}$; Run-off $212.4 \text{ m}^3/\text{sec}$.

flow with values of $K_z = 10 \text{ cm}^2/\text{sec}$ and $K_z = 25 \text{ cm}^2/\text{sec}$, respectively. In the latter case, vertical homogeneity is approached, and it is seen that substantial gravitational circulation can be maintained with a 6% top-to-bottom salinity difference.

Case V is shown in Figure 10. Variable eddy coefficients were used, but only the depth dependence as portrayed in Figure 4 was considered. A value of $KM = 10 \text{ cm}^2/\text{sec}$ was selected. In Figure 11 vertical means of the salinity values versus horizontal distance is plotted for Cases I through V. In addition, a salinity plot for September 10, 1962 and October 1, 1963 from Hudson River data (Gieses and Barr, 1967) is included. Salinity distributions were identical for both years. A relatively constant run-off value of $141 \text{ m}^3/\text{sec}$ (5000 cfs) was observed at a location well above the salt intrusion region for the three months that preceded the sampling in both cases. This value is slightly lower than the value used in the model and can be considered a typical value for low run-off conditions for the Hudson River Basin in late summer.

At least for the Hudson River, coefficients equal to $4 \text{ cm}^2/\text{sec}$ overestimate the salt intrusion. Doubling the vertical eddy viscosity coefficient (Case II) is seen to have a significant effect in reducing the length of intrusion. By consideration of the vorticity equation, it is seen that a larger value for the eddy viscosity is capable of supporting a steeper salinity gradient ($\partial S/\partial x$). This effect is again noticed in contrasting Case III (constant coefficients of $10 \text{ cm}^2/\text{sec}$) with Case V ($KM = 10 \text{ cm}^2/\text{sec}$, but decreasing near the bottom).

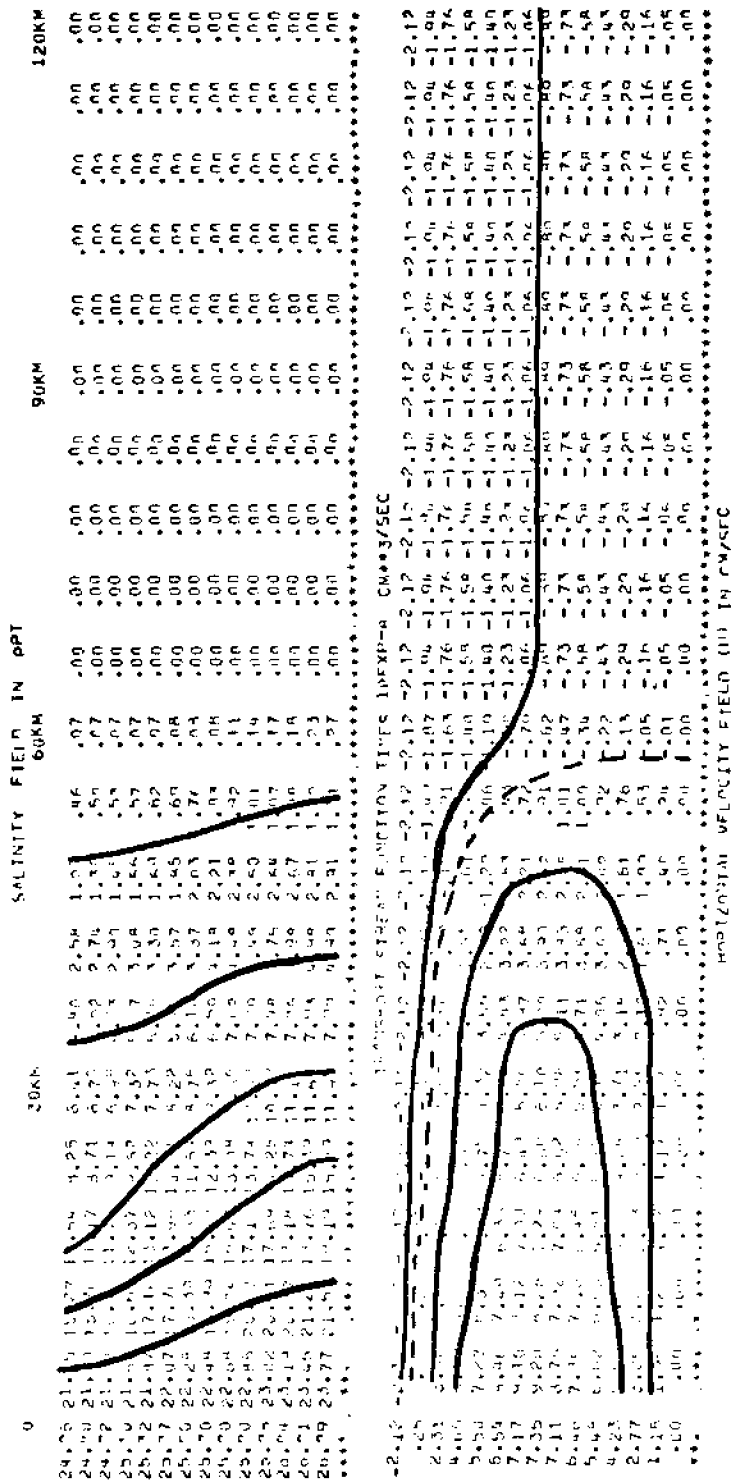


Figure 10. Case V. Variable coefficients without stability dependence; KM = 10cm²/sec; Run-off 212.4 m³/sec.

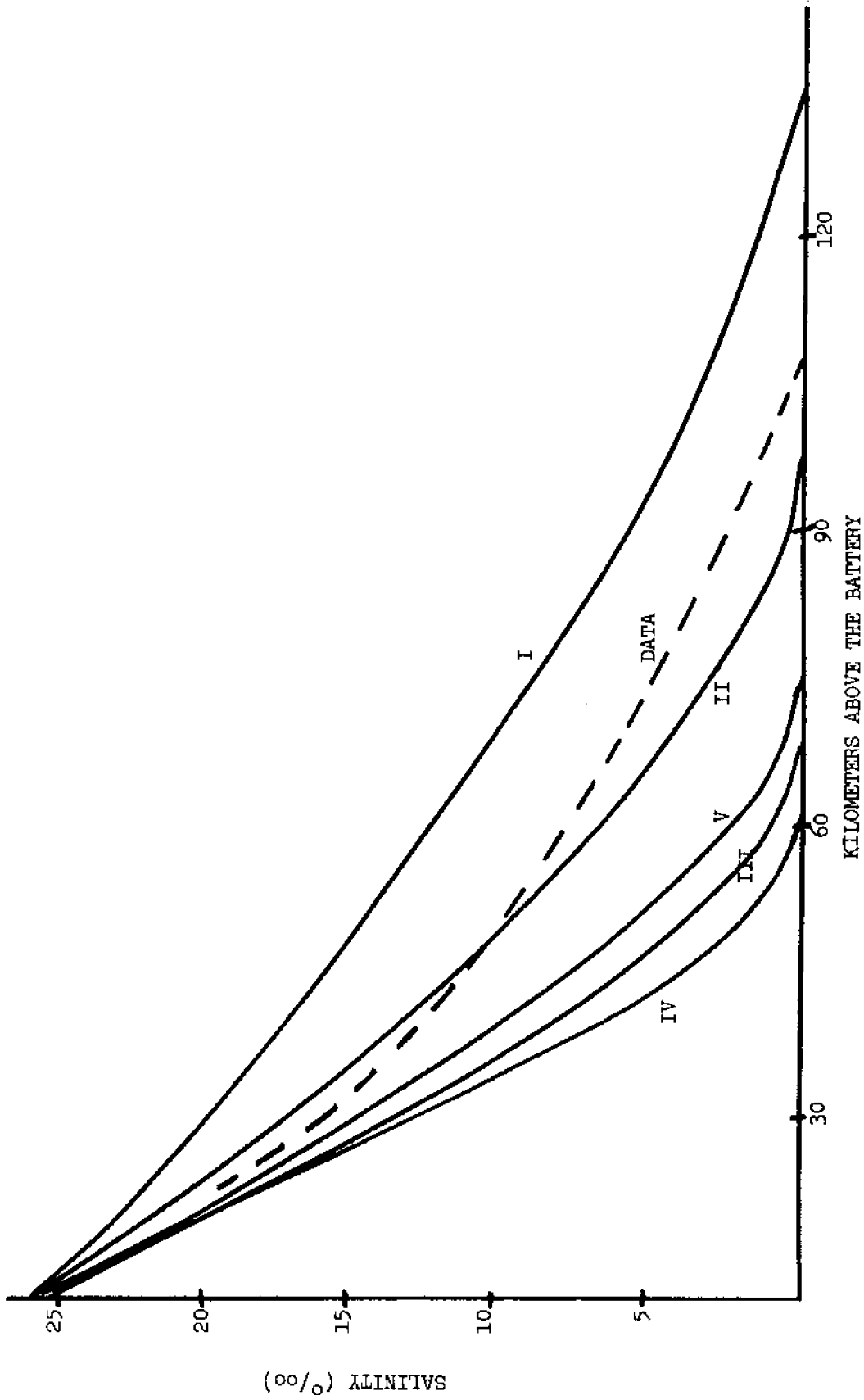


Figure 11. Plot of salinity versus distance into the estuary for Cases I-V. Cases I-V use increasing values of constant coefficients. Case V includes depth dependence for coefficients, but is without stability effects. Data corresponds to a low run-off condition for the Hudson River.

The remaining runs incorporate the full stability dependence of the eddy coefficients. New values for the coefficients at each grid point were computed each iteration after the new salinity field was determined. For these cases the steady state solution for coefficients decreasing with depth, but independent of stability (Case V) was used for initial values.

Cases VI, VII, VIII (Figures 12 to 14) show the full model under constant run-off as before ($212 \text{ m}^3/\text{sec}$, 7500 cfs), with three values for the maximum value of the eddy coefficients, $KM = 10, 15, 20 \text{ cm}^2/\text{sec}$. Comparison of Case VI with Case V, both with a value of $KM = 10 \text{ cm}^2/\text{sec}$, shows that the effect of stability significantly reduces the value of the coefficients and the intrusion length increases dramatically. The full model makes a qualitative improvement over the constant coefficient cases by tending to form a stronger halocline near mid-depth. Figure 15 shows plots of the vertical mean salinity versus horizontal distance for these three cases.

The value for KM is seen to have a strong influence on intrusion. A plausible explanation is the nonlinear feedback of stability upon the eddy diffusivity. Increasing the vertical salinity gradient reduces the value of the mixing coefficient, K_z , which further inhibits vertical mixing. This is demonstrated by two extreme cases. For $KM = 10 \text{ cm}^2/\text{sec}$ but allowing $K_z \rightarrow 0$ instead of $K_z \rightarrow 2$ for $R_1 \rightarrow \infty$, the nonlinear coupling produced intense vertical salinity gradients near mid-depth that completely shut off all vertical mixing. This can be contrasted with Case VIII which has a high coefficient for adiabatic mixing ($KM = 20 \text{ cm}^2/\text{sec}$). Here, the mixing is intense, so that weak vertical salinity gradients are maintained

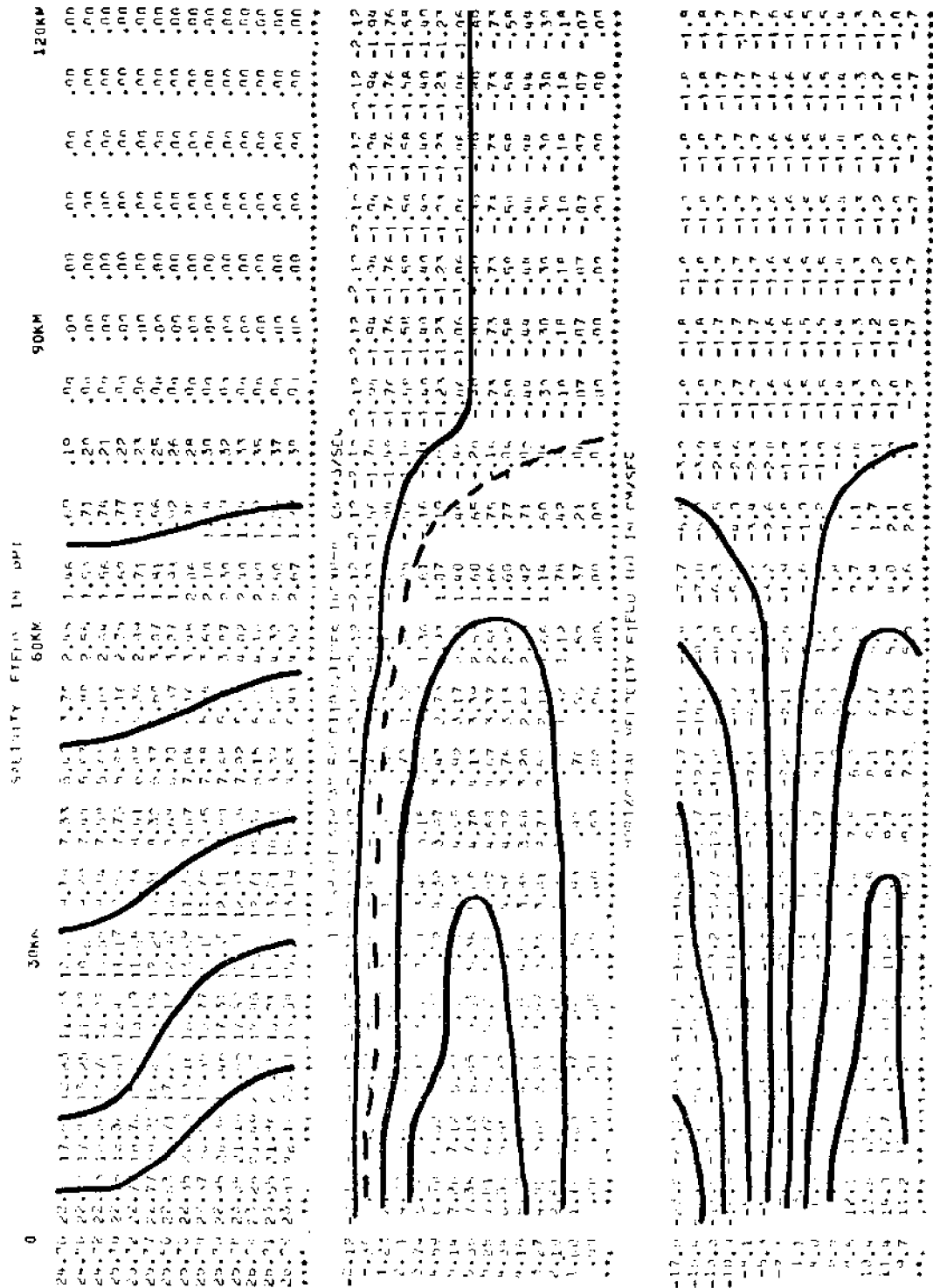


Figure 12. Case VI. Full model, KM = 10 cm²/sec; Run-off 212.4 m³/sec.

SALINITY FIELD IN PPT

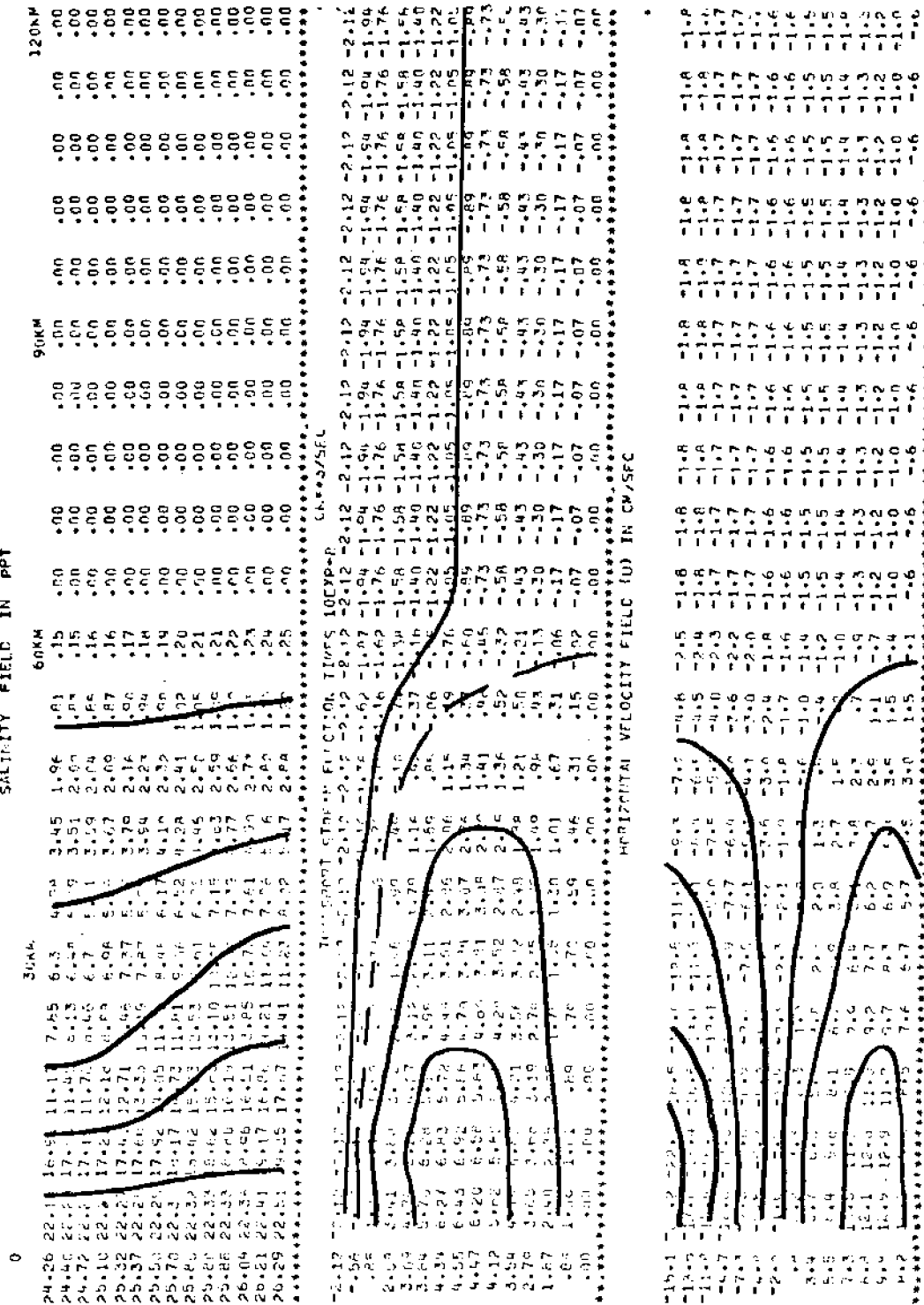


Figure 13. Case VII. Full model, KM = 15 cm²/sec; Run-off 212.4 m³/sec.

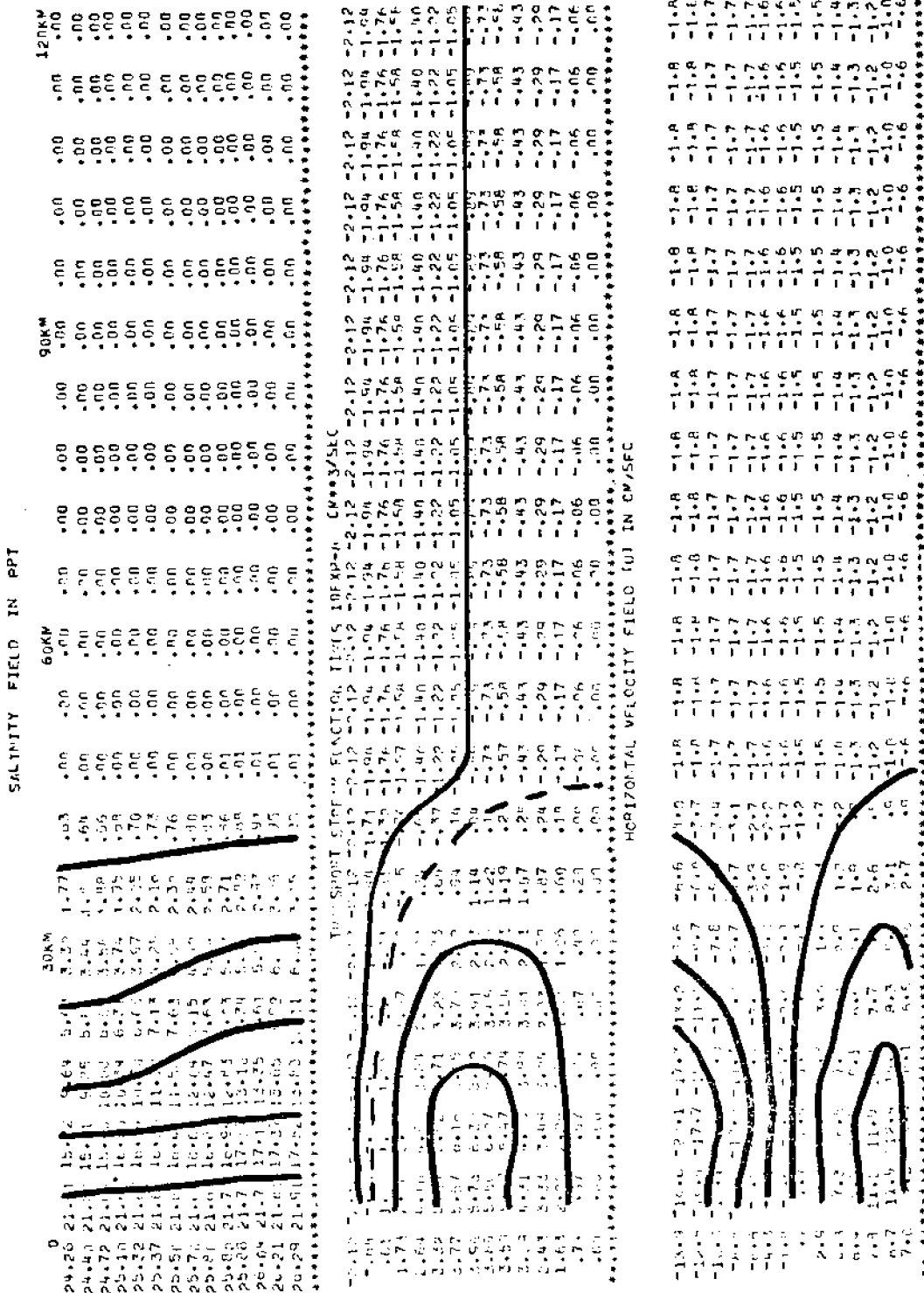


Figure 14. Case VIII. Full model, KM = 20 cm²/sec; Run-off 212.4 m³/sec.

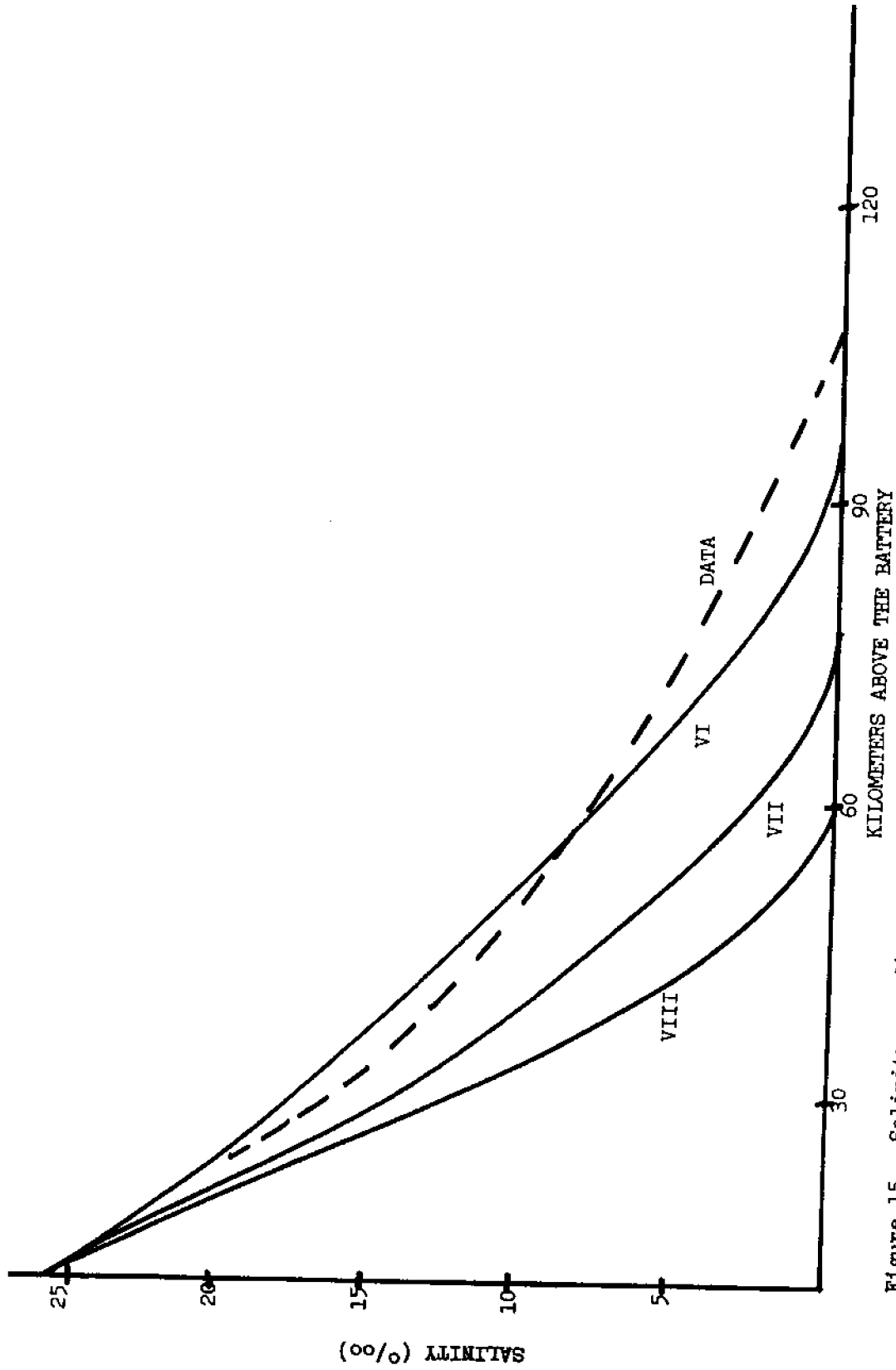


Figure 15. Salinity vs. distance into the estuary for Cases VI-VIII. These cases show the effect of varying the maximum eddy coefficient, KM, on salt intrusion. Cases VI, VII, VIII, correspond to KM values of 10, 15, 20 cm²/sec, respectively. Data is from Giese and Barr (1967). Model run-off was 7500 cfs (212.4 m³/sec).

by the vertical mixing coefficients. The magnitude of KM seems to lie in a range of 10 to 25 cm^2/sec and should be related to the local intensity of turbulent mixing. The range of observed coefficients (Table I) results from the lower KM values being reduced significantly by salinity stratification, while the high KM values are less affected. Thus, strong tidal straights such as the Hudson River and the Mersey River should have values for KM of 15 to 20 cm^2/sec or higher, while less intense regions, such as the James River, have values of about $KM = 10 \text{ cm}^2/\text{sec}$, which become strongly reduced by stratification effects.

Figures 16 and 17 show profiles for high ($424 \text{ m}^3/\text{sec}$, 15,000 cfs) and low ($99 \text{ m}^3/\text{sec}$, 3500 cfs) values of run-off (Cases IX and X) with $KM = 10 \text{ cm}^2/\text{sec}$. The mean horizontal salinity profiles are plotted in Figure 18 together with that for run-off equaling $212 \text{ m}^3/\text{sec}$ (Case VI). While there are considerable displacements of the salinity field for the three cases, the results suggest that one must make reasonable assumptions about mixing to determine the exact location of the limit of intrusion.

Two cases were also run with a run-off value of $141 \text{ m}^3/\text{sec}$ (5000 cfs). One assumed a KM equal to $15 \text{ cm}^2/\text{sec}$ (Case XI, Figure 19) and in the other KM equaled $20 \text{ cm}^2/\text{sec}$ (Case XII, Figure 20). Vertical mean salinity as a function of horizontal distance are shown in Figure 21 along with the measurements of Giese and Barr (1967).

It has been noted that the salinity field may move upstream under the action of southwest winds (Giese and Barr, 1967). In addition, Hansen and Rattray's model (1965) shows a strong dependence on wind effects.

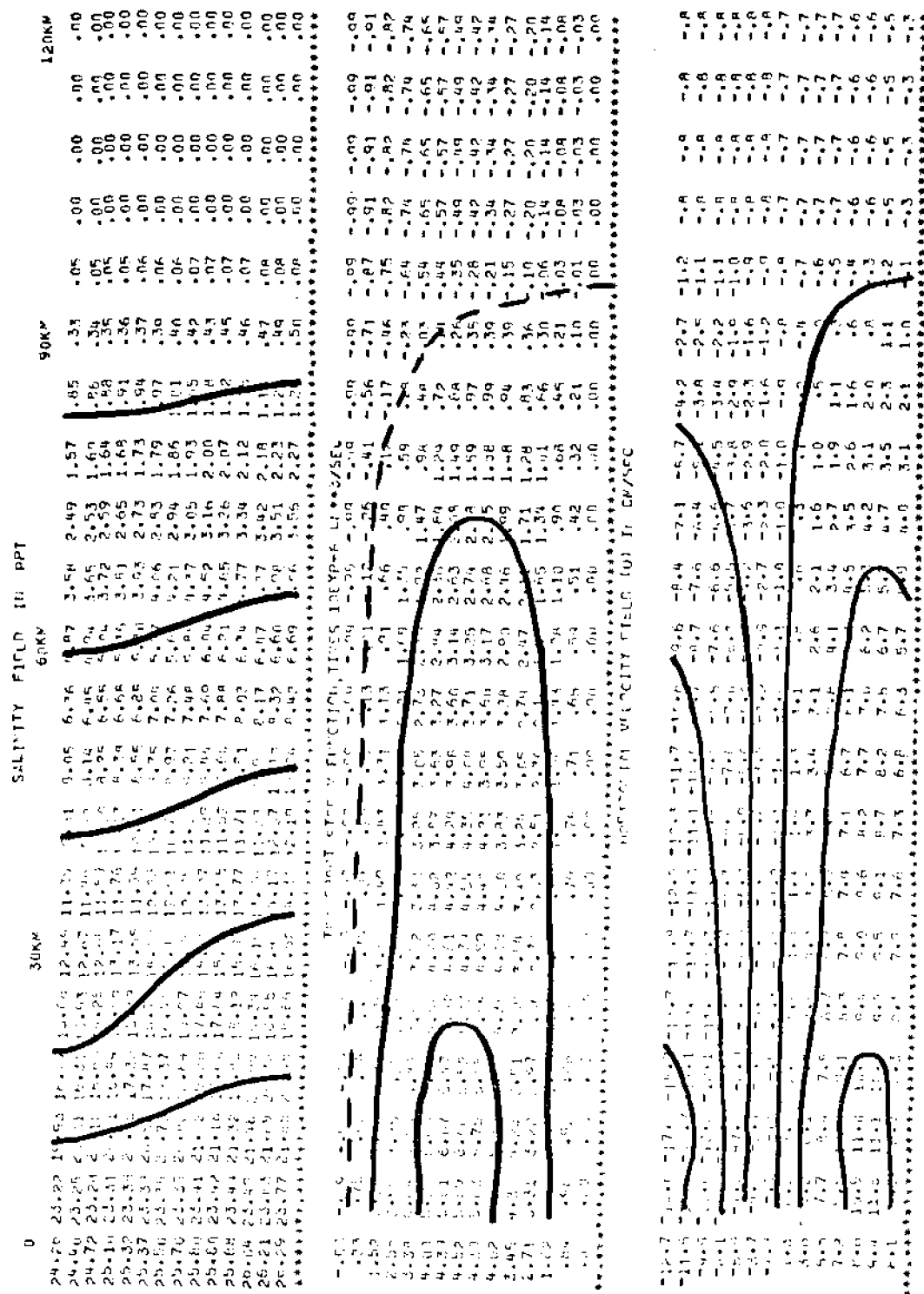


Figure 16. Case IX. Full model with low run-off.
 KM = 10 cm²/sec; Run-off 99.1 m³/sec.

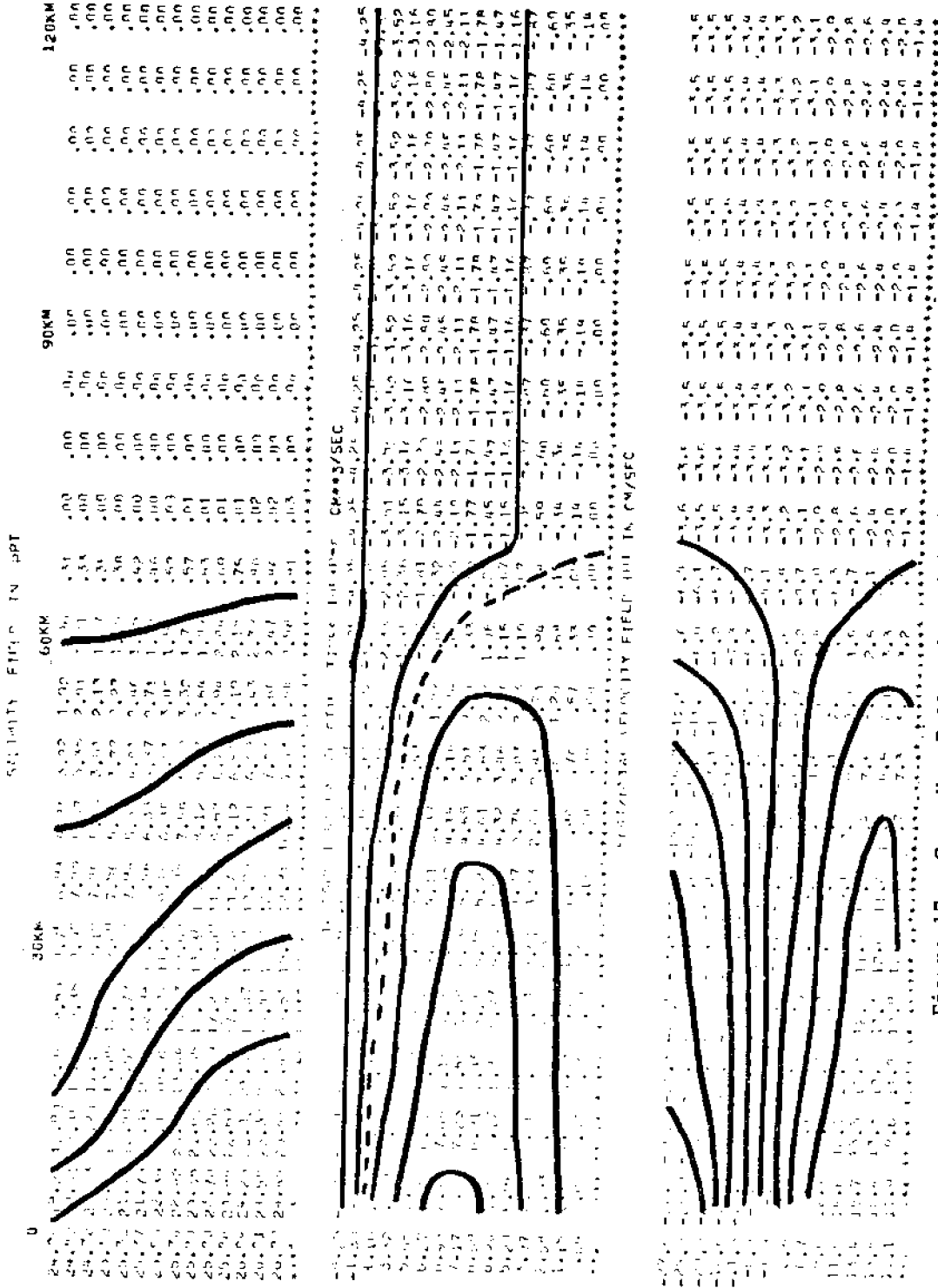


Figure 17. Case X. Full model with high run-off.
 KM = 10 cm²/sec; Run-off 424.8 m³/sec.

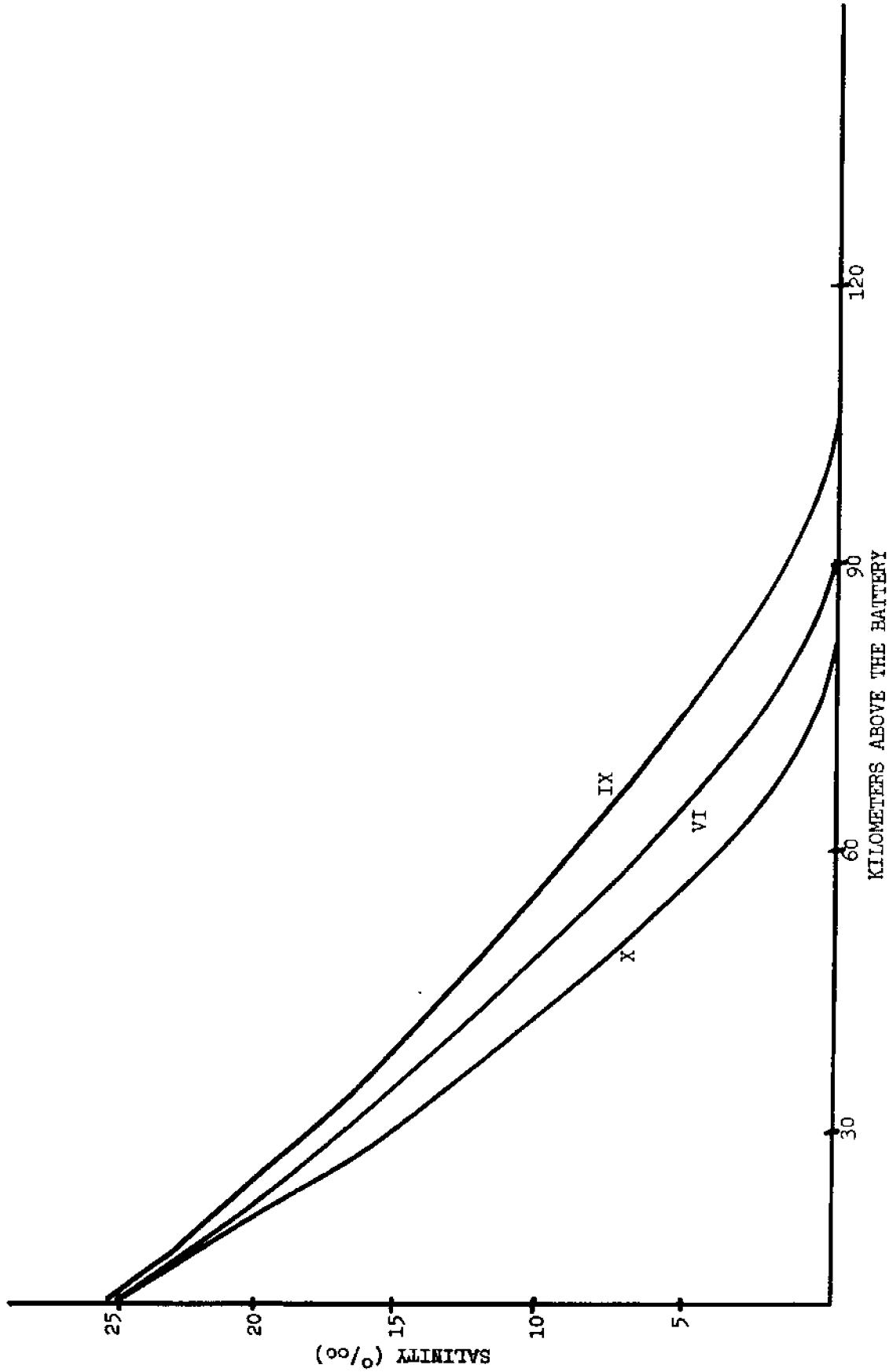


Figure 18. Salinity vs. distance into the estuary for Cases VI, IX, and X. With $KM = 10 \text{ cm}^2/\text{sec}$ plots show intrusion for run-off values of 3500, 7500, 15,000 cfs. (99.1, 212.4, 424.8 m^3/sec).

SALINITY FIELD IN PPT

| 0 | 30KP | 60KM | 90KP | 120KW | | | | | | | | | | |
|-------|-------|-------|------|-------|-------|------|------|------|------|-----|-----|-----|-----|-----|
| 24.26 | 18.37 | 3.22 | 8.59 | 7.56 | 6.04 | 4.44 | 2.93 | 1.60 | .64 | .00 | .00 | .00 | .00 | .00 |
| 24.40 | 22.17 | 18.40 | 3.42 | 8.84 | 7.74 | 6.15 | 4.55 | 2.97 | 1.64 | .65 | .00 | .00 | .00 | .00 |
| 24.72 | 22.49 | 18.43 | 3.65 | 10.12 | 7.95 | 6.24 | 4.63 | 3.02 | 1.64 | .66 | .00 | .00 | .00 | .00 |
| 25.10 | 22.60 | 18.50 | 3.92 | 10.45 | 8.21 | 6.34 | 4.72 | 3.08 | 1.69 | .68 | .00 | .00 | .00 | .00 |
| 25.32 | 22.71 | 18.59 | 4.27 | 10.91 | 8.56 | 6.45 | 4.85 | 3.16 | 1.74 | .70 | .00 | .00 | .00 | .00 |
| 25.47 | 22.70 | 18.70 | 4.67 | 11.47 | 9.01 | 6.93 | 5.01 | 3.25 | 1.74 | .72 | .00 | .00 | .00 | .00 |
| 25.50 | 22.71 | 18.82 | 5.10 | 12.07 | 9.51 | 7.24 | 5.19 | 3.36 | 1.84 | .75 | .00 | .00 | .00 | .00 |
| 25.70 | 22.71 | 18.94 | 5.53 | 12.66 | 10.01 | 7.57 | 5.37 | 3.46 | 1.90 | .77 | .00 | .00 | .00 | .00 |
| 25.80 | 22.73 | 19.05 | 5.94 | 13.14 | 10.48 | 7.88 | 5.52 | 3.57 | 1.96 | .80 | .00 | .00 | .00 | .00 |
| 25.80 | 22.74 | 19.13 | 6.25 | 13.62 | 10.85 | 8.15 | 5.73 | 3.67 | 2.01 | .82 | .00 | .00 | .00 | .00 |
| 25.98 | 22.74 | 19.22 | 6.51 | 13.94 | 11.11 | 8.37 | 5.87 | 3.75 | 2.06 | .84 | .00 | .00 | .00 | .00 |
| 26.04 | 22.75 | 19.32 | 6.74 | 14.22 | 11.41 | 8.57 | 6.00 | 3.83 | 2.10 | .86 | .00 | .00 | .00 | .00 |
| 26.21 | 22.76 | 19.45 | 7.00 | 14.51 | 11.68 | 8.79 | 6.15 | 3.93 | 2.14 | .88 | .00 | .00 | .00 | .00 |
| 26.79 | 22.77 | 19.56 | 7.18 | 14.69 | 11.85 | 8.93 | 6.26 | 3.99 | 2.19 | .90 | .00 | .00 | .00 | .00 |

TRANSPORT STREAM FUNCTION TIMES 10EXP-R U=3.75FL

| | | | | | | | | | | | | | | |
|-------|-------|-------|-------|-------|-------|-------|-------|-------|-------|-------|-------|-------|-------|-------|
| -1.42 | -1.42 | -1.42 | -1.42 | -1.42 | -1.42 | -1.42 | -1.42 | -1.42 | -1.42 | -1.42 | -1.42 | -1.42 | -1.42 | -1.42 |
| 1.11 | 1.94 | 2.57 | 3.55 | 4.84 | 6.44 | 8.34 | 10.54 | 13.04 | 15.84 | 18.94 | 22.44 | 26.34 | 30.64 | 35.34 |
| 1.07 | 1.08 | 1.09 | 1.10 | 1.11 | 1.12 | 1.13 | 1.14 | 1.15 | 1.16 | 1.17 | 1.18 | 1.19 | 1.20 | 1.21 |
| 2.08 | 3.20 | 3.71 | 3.27 | 2.90 | 1.91 | 1.44 | 1.08 | .64 | .43 | .40 | .33 | .27 | .21 | .17 |
| 2.91 | 4.24 | 4.89 | 4.38 | 3.96 | 2.93 | 1.71 | 1.15 | .82 | .53 | .40 | .33 | .27 | .21 | .17 |
| 3.52 | 4.63 | 5.33 | 4.84 | 4.19 | 3.39 | 2.77 | 2.08 | 1.54 | .83 | .64 | .51 | .40 | .33 | .27 |
| 3.91 | 5.52 | 6.19 | 5.68 | 4.83 | 3.80 | 3.13 | 2.50 | 1.81 | 1.06 | .83 | .70 | .58 | .46 | .35 |
| 4.06 | 5.64 | 6.26 | 5.71 | 4.74 | 3.96 | 3.20 | 2.64 | 1.95 | 1.18 | .84 | .70 | .58 | .46 | .35 |
| 3.95 | 5.43 | 5.96 | 5.45 | 4.60 | 3.87 | 3.23 | 2.61 | 1.95 | 1.21 | .85 | .70 | .58 | .46 | .35 |
| 3.63 | 5.04 | 5.33 | 4.82 | 4.17 | 3.54 | 2.94 | 2.42 | 1.82 | 1.15 | .87 | .72 | .60 | .48 | .36 |
| 3.42 | 4.19 | 4.46 | 4.07 | 3.51 | 3.01 | 2.55 | 2.02 | 1.57 | 1.02 | .83 | .71 | .59 | .47 | .35 |
| 2.45 | 3.24 | 3.39 | 3.08 | 2.68 | 2.33 | 1.93 | 1.63 | 1.24 | .81 | .66 | .56 | .46 | .36 | .28 |
| 1.64 | 2.14 | 2.19 | 1.88 | 1.54 | 1.24 | .93 | 1.32 | 1.09 | .84 | .66 | .56 | .46 | .36 | .28 |
| .75 | .76 | .95 | .86 | .77 | .68 | .59 | .49 | .38 | .26 | .12 | .01 | .00 | .00 | .00 |
| .00 | .00 | .00 | .00 | .00 | .00 | .00 | .00 | .00 | .00 | .00 | .00 | .00 | .00 | .00 |

HORIZONTAL VELOCITY FIELD (U) IN CM/SEC

| | | | | | | | | | | | | | | |
|-------|-------|-------|-------|-------|------|------|------|------|------|------|------|------|------|------|
| -12.6 | -16.9 | -14.8 | -17.0 | -9.0 | -7.4 | -9.0 | -7.4 | -9.0 | -7.4 | -9.0 | -7.4 | -9.0 | -7.4 | -9.0 |
| -11.3 | -16.5 | -15.1 | -17.6 | -10.7 | -9.4 | -8.1 | -6.8 | -5.5 | -3.6 | -1.7 | -1.2 | -1.2 | -1.2 | -1.2 |
| -9.8 | -12.6 | -14.1 | -13.1 | -11.1 | -9.5 | -8.3 | -7.1 | -5.8 | -4.4 | -3.0 | -1.5 | -1.2 | -1.2 | -1.2 |
| -8.0 | -10.4 | -11.4 | -13.7 | -7.3 | -8.1 | -7.0 | -6.0 | -4.9 | -3.8 | -2.6 | -1.4 | -1.1 | -1.1 | -1.1 |
| -5.9 | -7.5 | -8.1 | -7.7 | -7.0 | -6.2 | -5.4 | -4.6 | -3.8 | -3.0 | -2.2 | -1.3 | -1.1 | -1.1 | -1.1 |
| -3.8 | -4.7 | -5.0 | -4.2 | -4.0 | -3.5 | -3.1 | -2.6 | -2.1 | -1.7 | -1.2 | -1.1 | -1.1 | -1.1 | -1.1 |
| -1.4 | -1.2 | -1.7 | -1.3 | -1.3 | -1.5 | -1.4 | -1.3 | -1.2 | -1.2 | -1.1 | -1.1 | -1.1 | -1.1 | -1.1 |
| .00 | .00 | .00 | .00 | .00 | .00 | .00 | .00 | .00 | .00 | .00 | .00 | .00 | .00 | .00 |
| 3.1 | 4.9 | 5.0 | 4.2 | 3.2 | 2.5 | 1.9 | 1.3 | .9 | .5 | .1 | .0 | .0 | .0 | .0 |
| 4.9 | 7.2 | 8.5 | 7.9 | 6.1 | 4.1 | 3.3 | 2.3 | 1.3 | .7 | .7 | .9 | .9 | .9 | .9 |
| 6.5 | 8.1 | 9.5 | 9.5 | 7.9 | 6.6 | 5.4 | 4.4 | 3.2 | 2.0 | .7 | .6 | .9 | .9 | .9 |
| 7.8 | 10.6 | 11.6 | 10.1 | 9.1 | 7.7 | 6.4 | 5.0 | 3.9 | 2.5 | 1.0 | .4 | .8 | .8 | .8 |
| 8.6 | 11.4 | 11.9 | 10.3 | 9.4 | 8.2 | 7.0 | 5.7 | 4.4 | 2.9 | 1.3 | .3 | .7 | .7 | .7 |
| 7.2 | 9.3 | 9.2 | 8.3 | 7.4 | 6.6 | 5.7 | 4.8 | 3.7 | 2.5 | 1.2 | .1 | .4 | .4 | .4 |

Figure 19. Case XI. Full model, KM = 15 cm²/sec. Run-off 141.6 m³/sec.

| D | 30KM | | | 60KM | | | 90KM | | | 120KM | | |
|-------|----------|-------|--------|----------|-------|--------|----------|-------|--------|----------|-------|--------|
| | SALINITY | FIELD | IN PPT | SALINITY | FIELD | IN PPT | SALINITY | FIELD | IN PPT | SALINITY | FIELD | IN PPT |
| 24.76 | 21.00 | 17.33 | 11.63 | 7.55 | 1.95 | 2.06 | 1.50 | .00 | .00 | .00 | .00 | .00 |
| 24.90 | 22.00 | 17.12 | 11.08 | 7.52 | 1.92 | 1.94 | 1.48 | .00 | .00 | .00 | .00 | .00 |
| 24.92 | 22.00 | 17.34 | 7.14 | 6.91 | 1.87 | 1.92 | 1.56 | .00 | .00 | .00 | .00 | .00 |
| 25.10 | 22.00 | 17.35 | 7.23 | 6.23 | 1.83 | 1.90 | 1.50 | .00 | .00 | .00 | .00 | .00 |
| 25.12 | 22.00 | 17.30 | 7.56 | 6.53 | 1.85 | 1.88 | 1.51 | .00 | .00 | .00 | .00 | .00 |
| 25.17 | 22.00 | 17.40 | 7.84 | 6.80 | 1.87 | 1.89 | 1.52 | .00 | .00 | .00 | .00 | .00 |
| 25.20 | 22.11 | 17.54 | 7.12 | 6.26 | 1.84 | 1.76 | 1.58 | .00 | .00 | .00 | .00 | .00 |
| 25.30 | 22.11 | 17.53 | 7.41 | 6.55 | 1.83 | 1.83 | 1.55 | .00 | .00 | .00 | .00 | .00 |
| 25.40 | 22.16 | 17.56 | 7.93 | 6.82 | 1.86 | 1.86 | 1.57 | .00 | .00 | .00 | .00 | .00 |
| 25.50 | 22.20 | 17.87 | 7.10 | 6.56 | 1.87 | 1.90 | 1.58 | .00 | .00 | .00 | .00 | .00 |
| 25.64 | 22.22 | 17.96 | 7.28 | 6.77 | 1.87 | 1.92 | 1.60 | .00 | .00 | .00 | .00 | .00 |
| 25.71 | 22.22 | 18.06 | 7.43 | 6.93 | 1.87 | 1.92 | 1.62 | .00 | .00 | .00 | .00 | .00 |
| 25.79 | 22.25 | 18.15 | 7.53 | 7.03 | 1.87 | 1.92 | 1.63 | .00 | .00 | .00 | .00 | .00 |

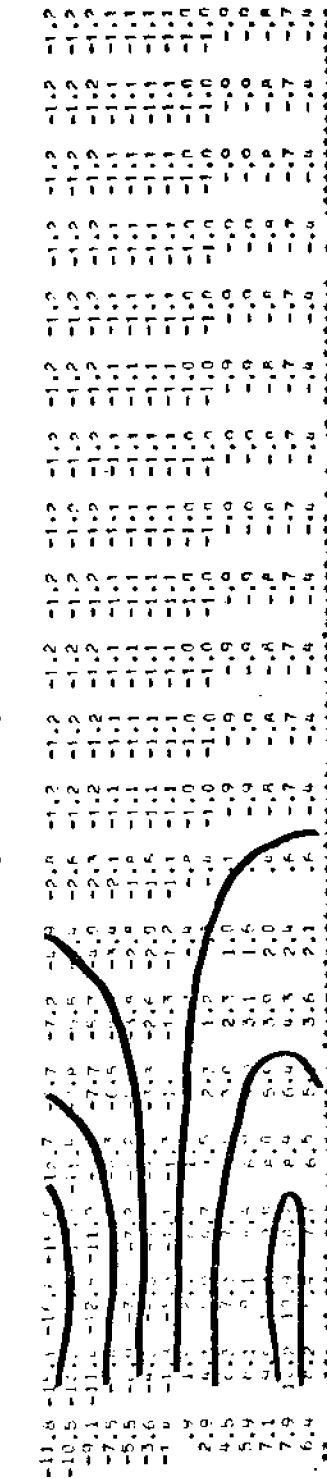
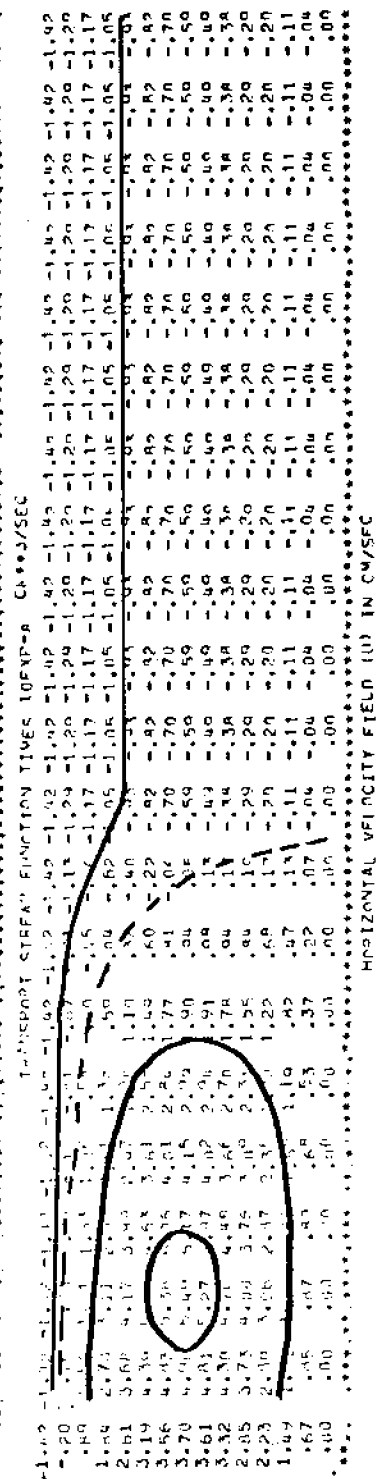


Figure 20. Case XII. Full model, KM = 20 cm²/sec; Run-off 141.6 m³/sec.

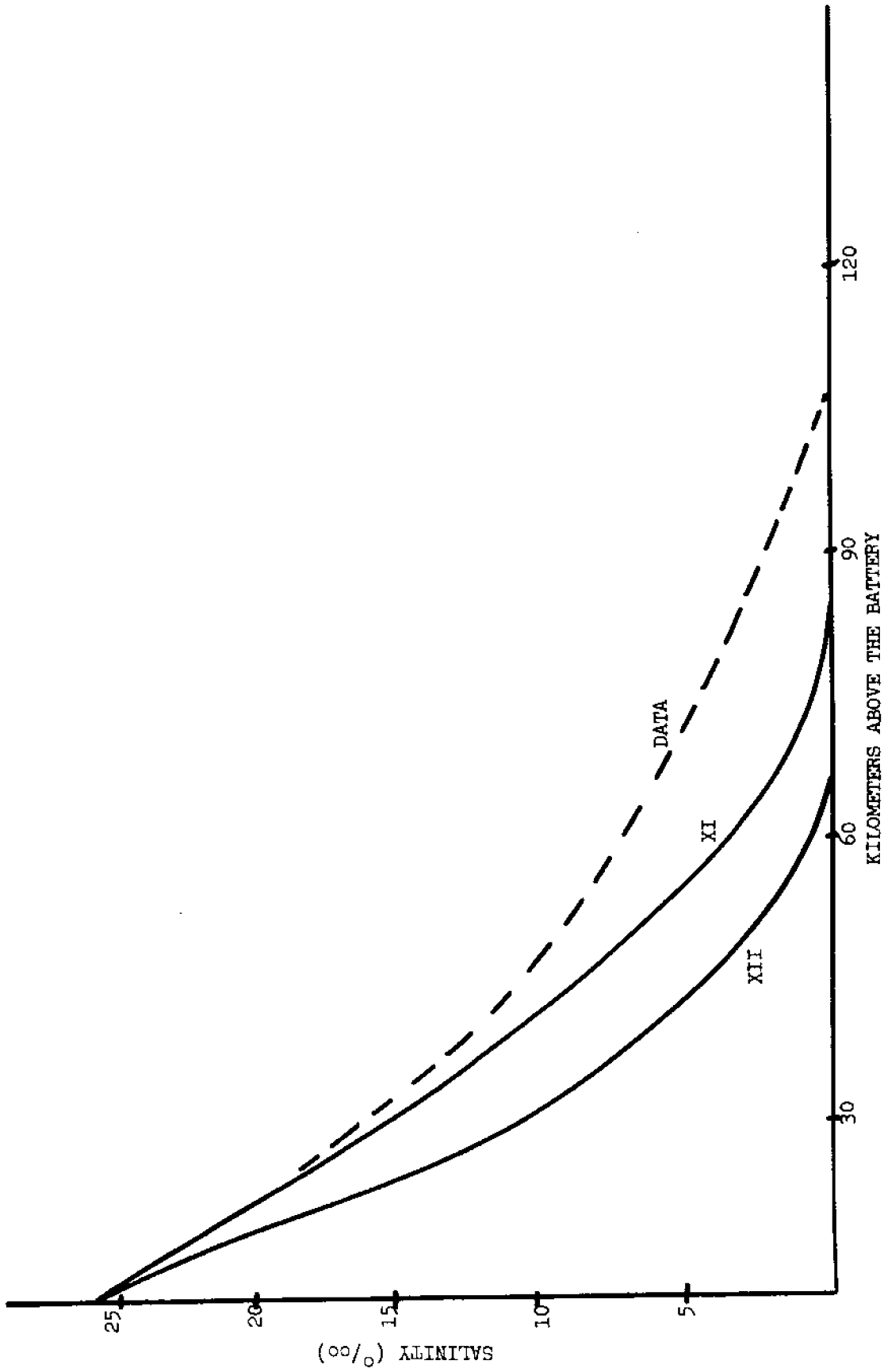


Figure 21. Salinity vs. distance into the estuary for Cases XI and XII. Case XI assumed a value of $15 \text{ cm}^2/\text{sec}$ for KM and Case XII assumed $20 \text{ cm}^2/\text{sec}$. Run-off was 5000 cfs ($141.6 \text{ m}^3/\text{sec}$).

Case XIII applied a constant wind stress of 0.1 dyne/cm^2 to the surface in the upstream direction. The result is shown in Figure 22 and should be compared to calm conditions (Case VI, Figure 12). Note the positive velocity values near the surface beyond the limit of salt intrusion.

The response of the model displaced the salt field slightly in the seaward direction. This result points to a sensitivity in the model formulation when stress is applied along a boundary. Inspection of the surface boundary condition suggests one cause. The velocity shear at the surface is equal to τ/A and is thus strongly dependent on the value of the eddy viscosity at the surface. That these coefficients are themselves functions of wind speed is illustrated by the work of Neumann (1952) and Schmidt (1917). Although calculated for open water conditions, the following table (assuming density = 1 gm/cm^3) from Schmidt demonstrates this dependence.

| WIND SPEED | m/sec | 1 | 3 | 5 | 7 | 10 | 15 | 20 |
|------------|----------------------|-----|----|-----|-----|-----|------|------|
| A | cm ² /sec | (1) | 28 | 110 | 220 | 430 | 1000 | 1720 |

Thus, the assumed value of the surface eddy coefficient used both in Case XIII and in Hansen and Rattray (1965) appear to be too small and prevents the wind stress from influencing the deeper layers.

Another cause is the restriction imposed by the stream function formulation that requires specification of net transport between the surface and bottom boundaries. This condition requires that if the surface waters are driven upstream by the wind, the seaward transports in the lower layers must increase to maintain the vertically integrated

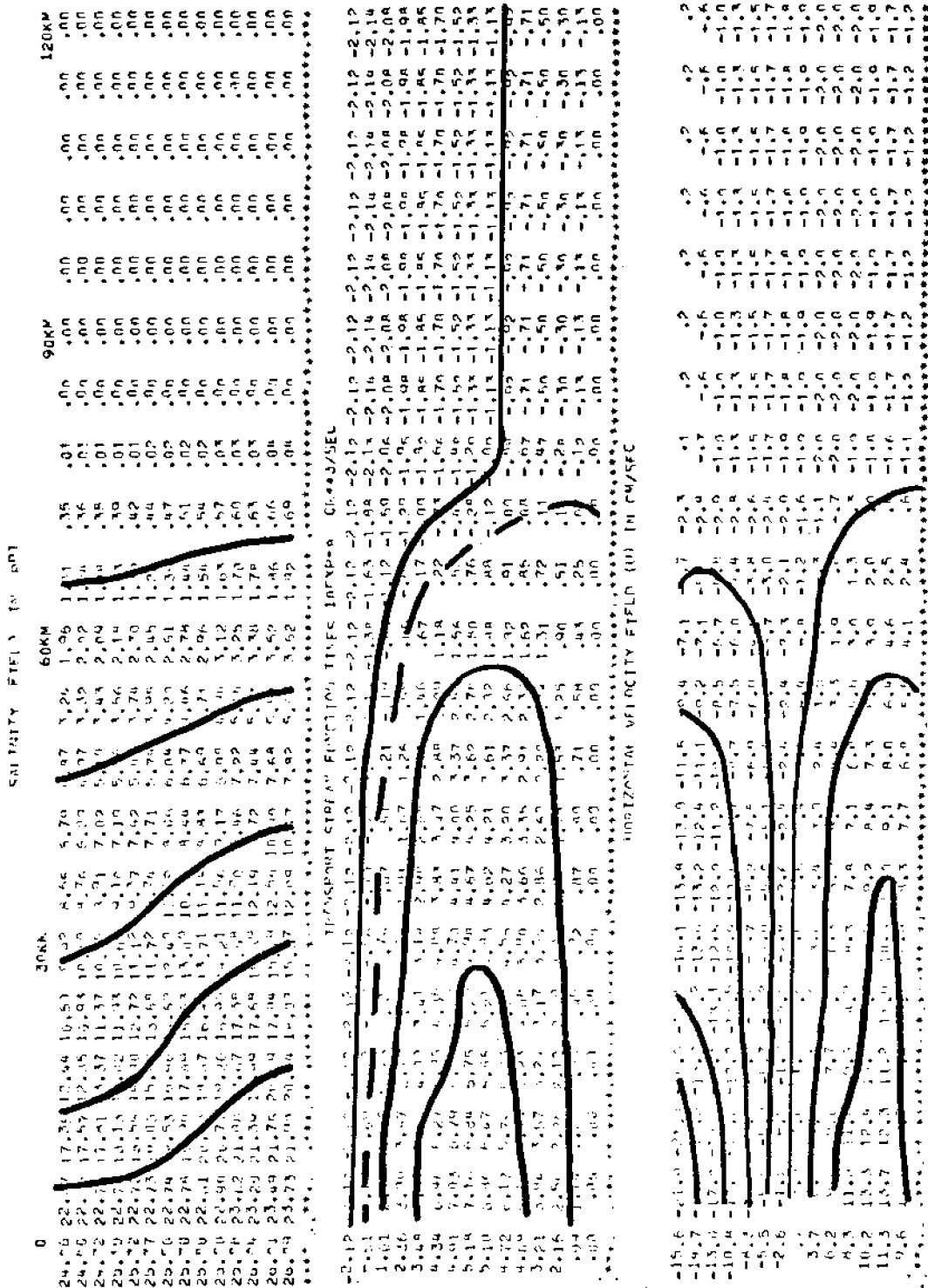


Figure 22. Case XIII. Wind stress results.

transport at a constant value. These higher transports in the lower layer are then more effective in opposing the salt influx, resulting in the slight seaward displacement of the salt field. While the seaward displacement may be physically realizable in some situations, the contrary evidence from the Hudson River indicated that there is a complex relationship between wind stress, river flow and vertical mixing that was not encompassed in the present model formulation.

V. EXAMPLES OF POLLUTANT LOADING

The spread of pollutants in an estuary is an exceedingly important problem and gives impetus to projects to improve the knowledge of estuary circulation.

The same type of separation into several dispersive modes obtained for salinity in Section I (Equation 1.4) may also be made by substituting any contaminant, C, in place of salinity, S. However, for the same geographic reaches, the various dispersion components for a contaminant may be of entirely different magnitudes than those for salt because each term is strongly dependent upon the cross sectional variation of the scalar in question. For example, at the initial release of a pollutant on one bank, the cross-channel gradient is sufficiently large so that the tidal dispersion term dominates. After a certain amount of time, however, the pollutant may approach lateral homogeneity and the convective circulation

component increases. Salinity is a special case because it is coupled with the motion field through density effects that minimize cross-channel variations and prohibit density inversions. Thus, it is not necessarily valid to infer dispersion characteristics for pollutants from salinity distributions, at least in partially mixed regions, or to assess the dispersion of salt assuming that it is a passive contaminant.

Two pollutant examples were run with the mean velocities obtained from the model: a point loading of a conservative contaminant and a continuous loading of a parameter able to diffuse across the free surface. Since the contaminants are considered passive, they do not interact with the motion field. The spread of the contaminants was calculated from the velocity and vertical mixing fields produced by the salt intrusion model (Case XI, Figure 19) which corresponds to late summer conditions in the Hudson River. The contaminant equation is a simple modification of the salt balance equation (3.12).

Figures 23 and 24 show the distribution for a slug loading of a conservative tracer for the initial condition, 1, 2, 7, 14 tidal cycles, and one month after the initial condition.

Figure 25 plots the mass in each section as a function of time. The initial condition is assumed to exist some time after original release so that the tracer is distributed uniformly across the channel and within the 6 kilometer segment and has a total relative mass of 1000. The seaward end is considered a sink so that any tracer reaching this point is removed by the tidal mixing of the lower harbor. After initial release, the effects

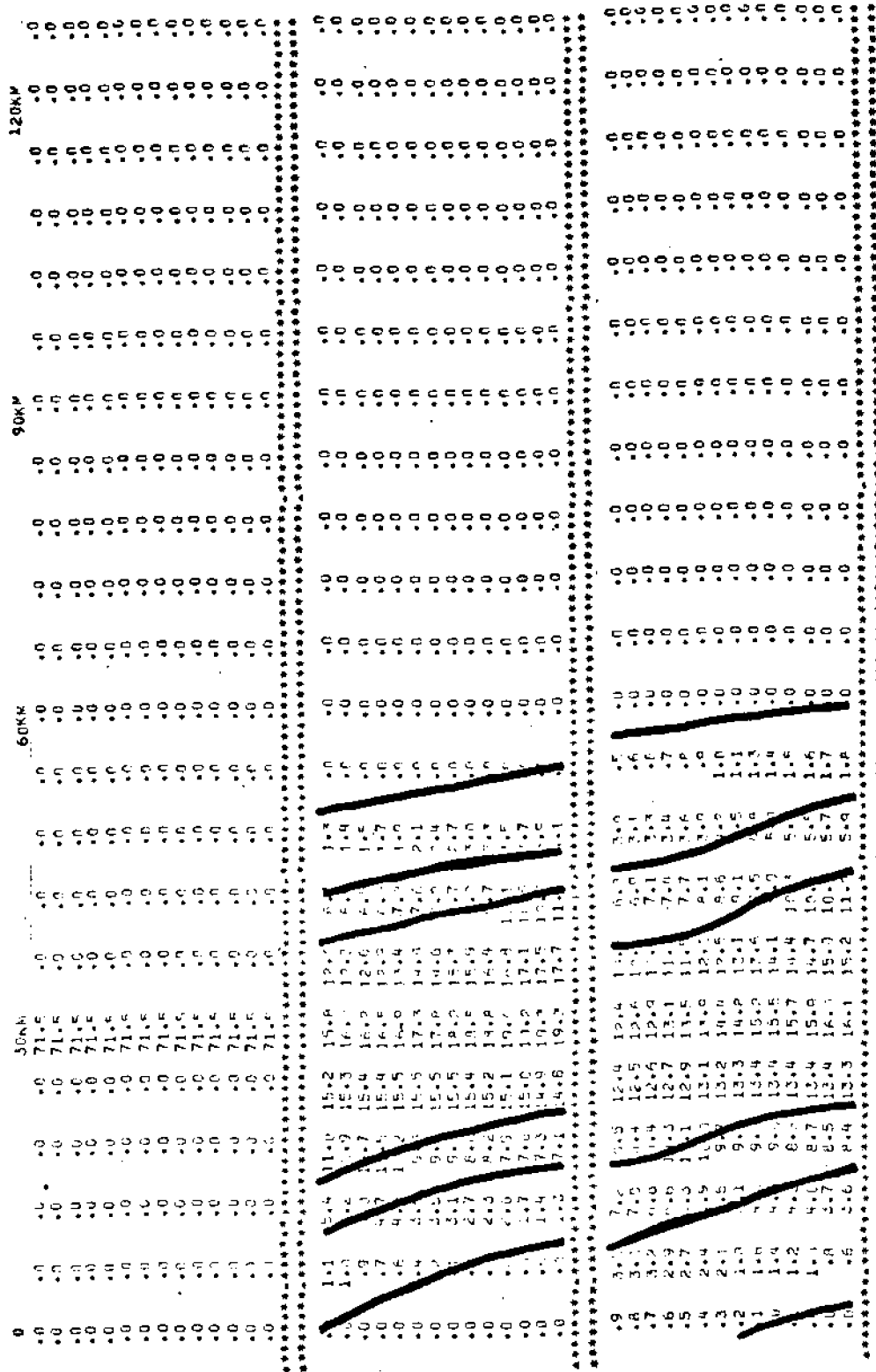


Figure 23. Distribution of a conservative tracer for initial condition, one tidal cycle (12.42 hrs) after the initial condition and two cycles. Contours are at 0, 5, and 10 relative units.

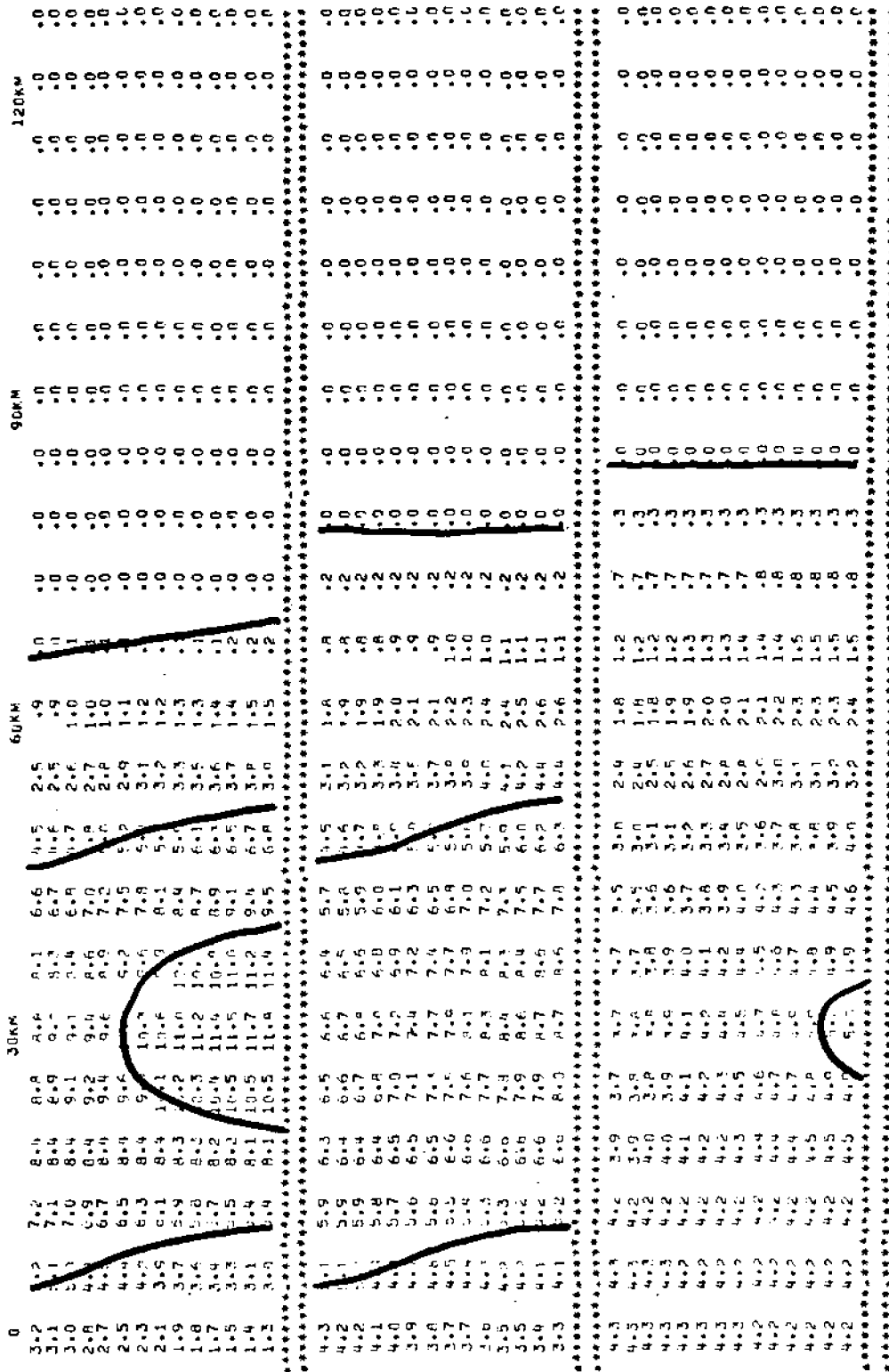


Figure 24. Distribution of a conservative tracer for seven and fourteen tidal cycles and one month after the initial condition. Contours are at 0, 5, 10 relative units.

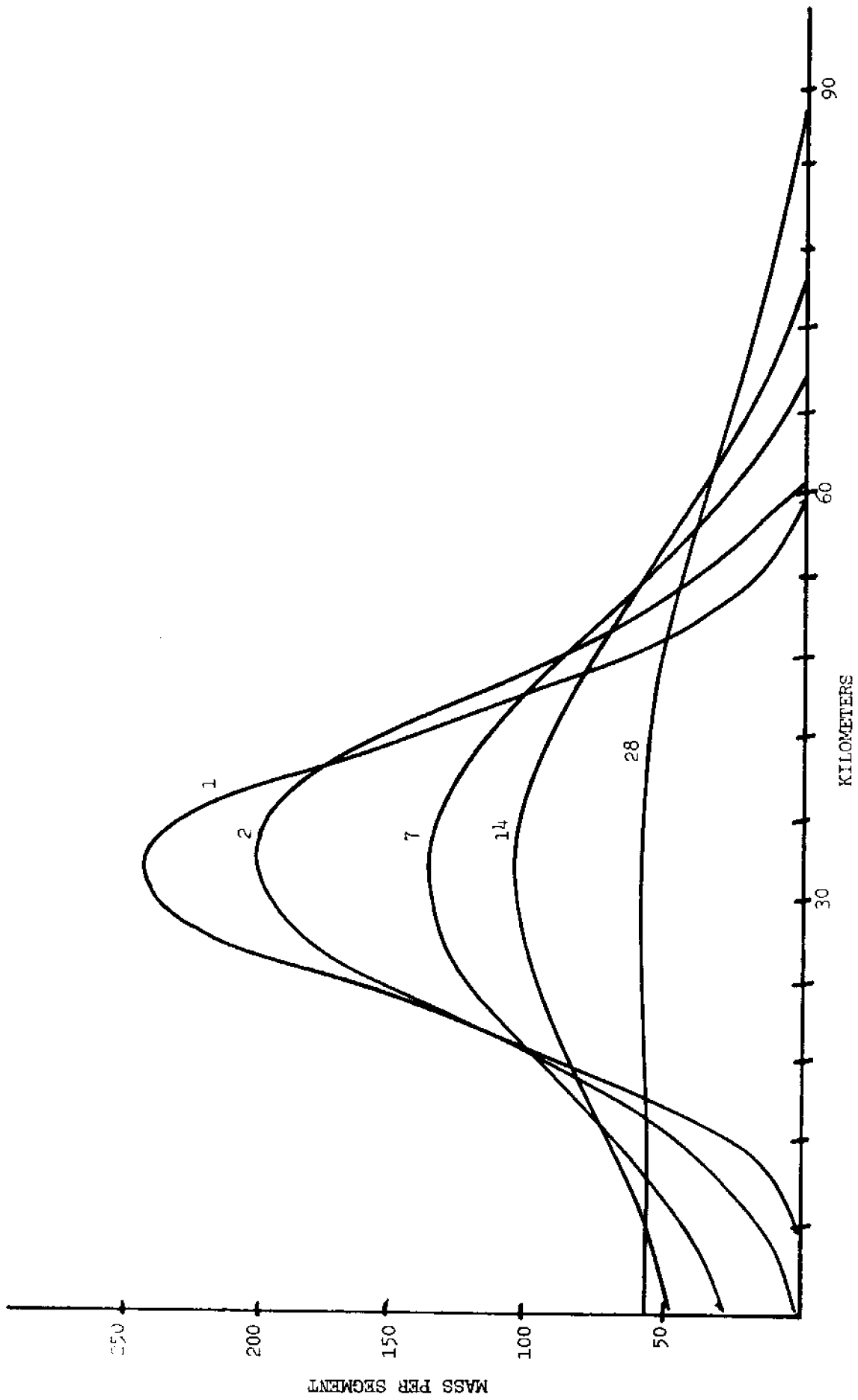


Figure 25. Plot of dye mass per 6 kilometer segment for 1, 2, 7, 14, 28 tidal cycles after release.

of the vertical shear are evident. There are high concentrations upstream of the release point near the bottom and downstream of the release point near the surface. As time progresses, the higher concentrations in the lower layers upstream of the release point diffuse toward the surface and are carried seaward in the surface layer. The tracer in the surface layer downstream from the release point diffuses toward the bottom and is carried back into the estuary. The net result is a large initial dispersion of the tracer, but within a few days a nearly closed circulation develops. This point is further emphasized by a plot of the total mass in the system versus time in Figure 26. Complete flushing requires several months and indicates that contaminants remain in the system for a long enough duration that their natural decay rates become important parameters.

It is instructive to compare this theoretical dye dump with actual dumps conducted by Hohman and Parke (1967) at eight locations in the Hudson River in August 1965. Run-off conditions were similar to those specified for the model run. Rhodamine B dye was dumped into the propeller wake of a boat traversing the river from bank to bank and the concentrations were monitored for 6 to 9 days. Above the salt intrusion region, the peak concentration of the dye patches were advected downstream about 16 km over 14 tidal cycles. The freshwater velocity of the model would predict a displacement of the order of 13 km. However, within the salt intrusion region, the dye concentration peak was stationary. Comparison with the model results shows that this feature is predicted

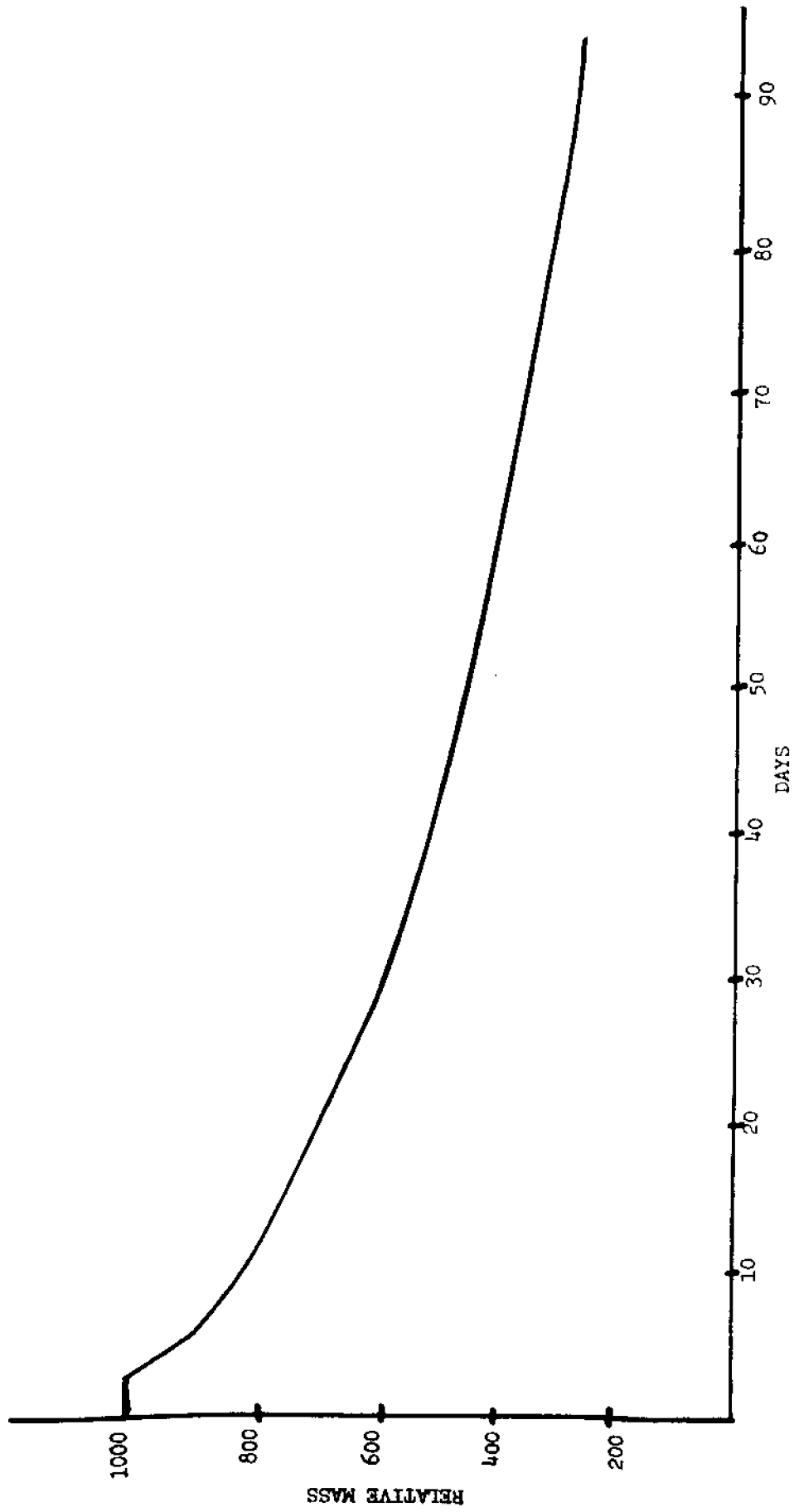


Figure 26. Amount of relative mass remaining in the system as a function of time. It required two days for traces of dump to reach the seaward limit of the model.

even for periods of a month or longer. Observed tidal excursions above and below the limit of salt intrusion were both of the order of 11 to 14 km. Both the results of the dye study and the results of the model indicate that the peak concentration is not advected downstream at the mean freshwater velocity in partially mixed regions as would be assumed with a one-dimensional simulation.

To calculate the apparent dispersion caused by the gravitational circulation, consider a contaminant equation of the following form

$$\frac{\partial c}{\partial t} = D_L \frac{\partial^2 c}{\partial x^2} \quad (5.1)$$

where D_L is a horizontal dispersion coefficient. This equation has the solution:

$$c = \frac{m}{\sqrt{4\pi D_L t}} \exp\left(-\frac{x^2}{4D_L t}\right) \quad (5.2)$$

where m is the total mass of dye dumped per unit cross section.

The dispersion coefficient can be calculated from the time dependence of the peak concentration.

$$D_L = \frac{m^2}{c_p^2 4\pi t} \quad (5.3)$$

where c_p is the maximum concentration at time t . D_L calculated from the model as a function of time is shown in the following table.

| TIME (DAYS) | .56 | 1.11 | 1.67 | 2.22 | 2.78 | 3.33 | 7.78 | 15.56 | 30.56 |
|---|------|------|------|------|------|------|------|-------|-------|
| $D_L \times 10^{-5} (\text{cm}^2/\text{sec})$ | 93.6 | 72.0 | 61.2 | 54.0 | 50.4 | 46.8 | 36.0 | 32.4 | 29.4 |

The decrease of D_L with time indicates the effect of recirculation. The D_L value of $36.0 \times 10^5 \text{ cm}^2/\text{sec}$ after 14 tidal cycles corresponds to Hohman and Parke's values of 7.5 to $22.0 \times 10^5 \text{ cm}^2/\text{sec}$. Agreement is close considering the use of a constant depth model and the errors inherent in dye studies. Values of the apparent dispersion coefficient are also reasonable compared to other estuaries as Bowden (1967) reports values of $16.1 \times 10^5 \text{ cm}^2/\text{sec}$ and $36.0 \times 10^5 \text{ cm}^2/\text{sec}$ for the Mersey Estuary.

The model corroborates the views of Eisenbud and Howells (1969) that the Hudson behaves as a brackish lake:

"Effluents and nutrients discharged into this brackish lake will, as in a true lake, be recirculated during a dry summer between water, sediments, and biota until irreversible eutrophication conditions are reached. Only the high spring flows provide a flushing volume of water necessary to prevent a continued accumulation of pollutants and eventual eutrophication."

The results for a continuous vertical line source of contaminant are shown in Figure 27 for .56, 3.3, and 9 days after the initial insertion of the loading. This example was run with the assumption that peak concentration of the contaminant in the river is continuously monitored so that the discharge rate is adjusted to maintain a pre-selected limit for the maximum allowable concentration. This was accomplished by reinitializing the concentration at the release point after each iteration. The contaminant was considered conservative and can diffuse across the free surface. The surface layer is able to diffuse heat and matter across the surface interface with an assumed turbulent diffusion coefficient of $K_z = 3 \text{ cm}^2/\text{sec}$. The gradient at the surface was estimated by differencing the concentrations a half meter above and below

the surface. The atmosphere is considered to be a sink with the relative concentration maintained at zero.

This example can be considered a loading of any anomalous value inserted into background conditions. It could represent the maintenance of a thermal plume which is 2 C warmer than the ambient water and air temperature, or an oxygen deficiency which is being replenished only by surface reaeration. It is assumed that salinity controls density so that no buoyancy effects are considered in the thermal discharge. Steady state conditions developed after eight days. The results indicate that the gravitational circulation acts to disperse the anomaly in the immediate vicinity of discharge, where it is acted upon by surface exchange. The sink for the anomaly is surface exchange rather than flushing of the system.

VI. CONCLUSION

A fourteen layer model for the circulation in partially mixed estuaries has been developed that is capable of assessing the response of horizontal and vertical variations of the salinity field to changes in run-off and turbulent mixing. The ability to perform a direct calculation of the dispersion of a pollutant due to vertical shear of the gravitational circulation has also been demonstrated. The model can now be applied to specific estuaries with the following procedure.

1. Reduce the horizontal grid spacing and include depth and width dependence. As the reduction in cross sectional area in the upstream direction reduces the volume per unit upstream horizontal distance, the total amount of salt that is necessary to maintain a certain concentration is decreased. This may explain why the Hudson River salinity data tapers off more gradually at the upstream face than predicted by the model.

2. A set of salinity observations including both vertical and upstream profile for late summer are necessary to tune the model.

3. Either through better understanding of the relation of turbulent energy to tidal currents or by fitting vertical salinity profiles, a value for KM should be determined for each horizontal segment.

4. Since tidal mixing contributes to the horizontal dispersion, the horizontal salinity profiles using KM from above may not match those observed. Increased tidal mixing is then estimated by making the horizontal smoothing operator (3.14) diffusive in order to match the observed horizontal profiles.

While this investigation did not finely tune the model to the Hudson River, and while some of the horizontal dispersion of the Hudson is of tidal origin, the conclusion that the gravitational circulation recycles imposed loads demonstrates the necessity of care when planning large fresh water diversions of the Hudson River or heavy pollutant loading during the summer.

Circulation modeling of broad, shallow, well mixed estuaries where vertical integration can be justified (see Leendertse, 1970, for example) is reasonably well established. This report has demonstrated the feasibility of resolving the important vertical variations in narrow partially mixed estuaries in the framework of a numerical model. However, several specific applications of the model are necessary to determine its suitability for practical problems in pollution modeling.

In more general situations, the three-dimensional tidal velocities are necessary to compute dispersion. Circulation models of these estuaries will require both large computer capability and an improvement of the theoretical understanding of vertical profiles of tidal currents.

REFERENCES

- Arakawa, A., 1966: Computational Design for Long-Term Numerical Integration of the Equations of Fluid Motion: Two Dimensional Incompressible Flow. Part 1. J. Comp. Phys. 1, pp. 119-143.
- Bowden, K.F., 1965: Horizontal mixing in the sea due to a shearing current. J. Fluid Mech., 21 (2) pp. 83-95.
- Bowden, K.F., 1967: Stability effects on turbulent mixing in tidal currents. Phys. Fluids, Supplement, p. S278
- Bowden, K.F., 1967: Circulation and diffusion, in Estuaries. A.A.A.S. Pub. 83, Washington, D.C.
- Bowden, K.F. and Sharef El Din, 1966: Circulation, salinity and river discharge in the Mersey estuary. Geophys. J. Roy. Astron. Soc., 10, pp. 383-399.
- Bowden, K.F. and R.M. Gilligan, 1971: Characteristic features of estuarine circulation as represented in the Mersey estuary. Lim. and Ocean, 16 (3), pp. 490-502.
- Bryan, K., 1963: A numerical investigation of a nonlinear model of a wind-driven ocean. J. Atm. Sci., 20, pp. 594-606.
- Bryan, K., 1969: A numerical method for the study of the circulation of the world ocean. J. of Comp. Phys., 4, pp. 347-376.
- Eisenbud, M. and G. P. Howells, 1969: Development of a biological monitoring system and a survey of trace metals, radionuclides and pesticide residues in the lower Hudson River. Institute of Environmental Medicine, New York University Medical Center.
- Fisher, J.S., J.D. Ditmars, and A.T. Ippen, 1972: Mathematical simulation of tidal time-averages of salinity and velocity profiles in estuaries. MIT Report #MITSG 72-11.
- Giese, G.L and J.W. Barr, 1967: The Hudson River Estuary: A preliminary investigation of flow and water quality characteristics. State of New York Conservation Dept., Water Resources Commission Bull. 61, 39 pp.
- Hansen, D.V., 1967: Salt balance and circulation in partially mixed estuaries in Estuaries, A.A.A.S. Pub. 83, Washington, D.C.
- Hansen, D.V., and M. Rattray, Jr., 1965: Gravitational circulation in straits and estuaries. J. Mar. Res., 23, pp. 104-122.
- Hansen, D. V. and M. Rattray, Jr., 1972: Estuarine circulation induced by diffusion. J. Mar. Res., 30, pp. 281-294.

- Haltiner, G.J., 1971: Numerical Weather Prediction. John Wiley and Son, Inc., New York.
- Hohman, M.H., D.B. Parke, 1967: Hudson River dye studies, in Hudson River Ecology. Hudson River Valley Commission.
- Kent, R.E. and D.W. Pritchard, 1959: A test of mixing length theories in a coastal plain estuary. J. Mar. Res., 18, p. 63.
- Kullenberg, G., 1972: Apparent horizontal diffusion in stratified vertical shear flow. Tellus, 24 (1), p. 17.
- Laasonen, P., 1949: Uber eine Method zur Losung der Warneleitungsgleichung. Acta Math, vol. 81, p. 309.
- Munk, W.H. and E.R. Anderson, 1948: Notes on a theory of the thermocline. J. Mar. Res., 7, pp. 276-295.
- Leendertse, J.J., 1970: A water-quality simulation model for well mixed estuaries and coastal seas: Volume 1, Principles of computation. Memo RM 6230, The Rand Corp., Santa Monica, Calif.
- Neumann, G., 1952: Uber die komplexe Natur des Seeganges. Teil 2, Deut. Hydrogr. Zeit., vol. 5, no. 5/6, pp. 252-277.
- Okubo, A., 1967: The effect of shear in an oscillatory current on horizontal diffusion from an instantaneous source. Int. J. Ocenol. and Limnol., 1, 3. p. 194.
- Overland, J.E., 1973: On the use of the DuFort-Frankel finite-difference approximation for simulation of diffusion in geophysical fluids. J. Phys. Ocean., Oct. 1973 (in press).
- Pritchard, D., 1956: The dynamic structure of a coastal plain estuary. J. Mar. Res., 15, p. 33.
- Pritchard, D.W., 1960: The movement and mixing of contaminants in tidal estuaries, in Proc. of the First International Conference on Waste Disposal in the Marine Environment, Pergamon Press.
- Rattray, M., Jr. and D. Hansen, 1962: A similarity solution for circulation in an estuary. J. Mar. Res., 20, pp. 121-133.
- Richtmyer, R.D. and K.W. Morton, 1967: Difference Methods for Initial Value Problems. Interscience, New York. 506pp.
- Schmidt, W., 1917: Wirkingen der ungeordneten Bewegungen im Wasser der Mure und Seen. Ann. de. Hydr. u. Marit. Meteorol., vol. 45, pp. 367-381 and 431-445.
- Taylor, G.I., 1954: The dispersion of matter in turbulent flow through a pipe. Proc. Roy. Soc., A. 223, pp. 446-468.